RESEARCH ARTICLE

MUCOSAL IMMUNOLOGY

Innate lymphoid cells regulate intestinal epithelial cell glycosylation

Yoshiyuki Goto,[1,2,3] Takashi Obata,[1,3] Jun Kunisawa,[1,4,5] Shintaro Sato,[1,2] Ivaylo I. Ivanov,[6] Aayam Lamichhane,[1] Natsumi Takeyama,[1,7] Mariko Kamioka,[1] Mitsuo Sakamoto,[3] Takahiro Matsuki,[8] Hiromi Setoyama,[8] Akemi Imaoka,[8] Satoshi Uematsu,[9,10] Shizuo Akira,[11] Steven E. Domino,[12] Paulina Kulig,[13] Burkhard Becher,[13] Jean-Christophe Renauld,[14] Chihiro Sasakawa,[7,15,16] Yoshinori Umesaki,[8] Yoshimi Benno,[17] Hiroshi Kiyono[1,2,5]

Fucosylation of intestinal epithelial cells, catalyzed by fucosyltransferase 2 (Fut2), is a major glycosylation mechanism of host–microbiota symbiosis. Commensal bacteria induce epithelial fucosylation, and epithelial fucose is used as a dietary carbohydrate by many of these bacteria. However, the molecular and cellular mechanisms that regulate the induction of epithelial fucosylation are unknown. Here, we show that type 3 innate lymphoid cells (ILC3) induced intestinal epithelial *Fut2* expression and fucosylation in mice. This induction required the cytokines interleukin-22 and lymphotoxin in a commensal bacteria–dependent and –independent manner, respectively. Disruption of intestinal fucosylation led to increased susceptibility to infection by *Salmonella typhimurium*. Our data reveal a role for ILC3 in shaping the gut microenvironment through the regulation of epithelial glycosylation.

In the gastrointestinal tract, bilateral regulation between the gut microbiota and the host creates a mutually beneficial environment. The intestinal epithelium is a physical barrier that separates the environments inside and outside the mucosal surface. Intestinal epithelial cells (ECs) are the first line of defense against foreign antigens, including those from commensal and pathogenic bacteria. ECs play key roles in initiating and maintaining an immunologically appropriate and balanced environment in reaction to constant foreign stimulation (*1*). Resident commensal bacteria support the development of this functional mucosal immune system, and in turn, mucosal immune cells control the homeostasis of the gut microbiota and protect against pathogenic bacterial infection through intestinal ECs. In particular, type 3 innate lymphoid cells (ILC3) produce interleukin-22 (IL-22), which not only regulates the homeostasis of the commensal microbiota but also protects against *Citrobacter rodentium* infection, presumably by inducing EC-derived antimicrobial molecules such as RegIIIγ (*2–5*).

Fucosylated carbohydrate moieties expressed on intestinal ECs are involved in the creation of an environmental niche for commensal bacteria in mice and humans (*6–10*). Fucosylated glycans are generated by the addition of an L-fucose residue via an α1-2 linkage to the terminal β-D-galactose residues of glycan in a process catalyzed by fucosyltransferase. Two fucosyltransferases, Fut1 and Fut2, mediate intestinal epithelial fucosylation, and each enzyme acts on a distinct subset of epithelial cells. Fut1 regulates fucosylation of Peyer's patch (PP) M cells, whereas Fut2 is a key enzyme regulating intestinal columnar epithelial fucosylation and the production of secretory fucosylated ABO(H) histo-blood group antigens (*11*). Defective Fut2 has been shown to result in susceptibility to *Candida albicans* infection in mice (*12*). In addition, inactivating polymorphisms of *FUT2* are associated with metabolic abnormalities and infectious and inflammatory diseases in humans (*13–19*).

The importance of epithelial fucose has been explored through studies of host–microbe interactions. Signals from commensal bacteria are required for epithelial fucosylation (*6*). Specific commensals, in particular *Bacteroides*, have been shown to induce epithelial fucosylation and are able to catabolize fucose for energy or incorporate it into bacterial cellular components—capsular polysaccharides—that give microbes a survival advantage in competitive environments (*8*, *9*). Indeed, a lack of Fut2 alters the diversity and composition of the fecal microbiota in humans and mice (*20*, *21*). Therefore, epithelial fucose functions as a mediator between the host and commensal microbiota. Although a previous report proposed a model in which *Bacteroides*–EC interaction mediates epithelial fucosylation (*7*), the precise mechanisms by which Fut2 regulates fucosylation remain largely unknown.

Microbiota induces epithelial fucosylation

Epithelial fucosylation, a major glycosylation process, occurs in the small intestine (*10*, *11*). To assess the inductive mechanism of intestinal epithelial fucosylation, we first investigated the localization of fucosylated ECs (F-ECs) along the length of the small intestine, divided equally into four parts from the duodenum (part 1) to the terminal ileum (part 4), in naïve mice (Fig. 1A). The frequency of F-ECs, detected with the α(1,2)-fucose-recognizing lectin *Ulex europaeus* agglutinin-1 (UEA-1), was low in the duodenum and jejunum (part 1 and a portion of part 2; <15% F-ECs) and gradually increased toward the ileum (part 4; 40 to 90% F-ECs) (Fig. 1, A to C). Consistent with epithelial fucosylation, epithelial Fut2 expression was also higher in the ileum (Fig. 1D). Because greater numbers of microorganisms are present in the distal ileum than in the duodenum (*22*), it may be possible that high numbers of ileal F-ECs are induced and maintained through microbial stimulation. To test this hypothesis, we examined the fucosylation status of ileal ECs (part 4) in mice treated with a mixture of antibiotics (AB), as well as in germ-free (GF) mice. The number of F-ECs was dramatically reduced in AB-treated and GF mice (Fig. 2A and fig. S1A). Furthermore, expression of epithelial *Fut2* was also reduced in AB-treated mice (Fig. 2B). Epithelial fucosylation was restored after cessation of AB treatment and in conventionalized GF mice (Fig. 2A and fig. S1A). In addition, fucosylation of goblet cells, but not Paneth cells, was lost in AB-treated and GF mice (Fig. 2C), indicating that commensal bacteria induce fucosylation of columnar epithelial cells and goblet cells, but not Paneth cells.

It has been shown that epithelial fucosylation can be induced by the mouse and human commensal *Bacteroides thetaiotaomicron* (*6*). However, on the basis of bacterial 16*S* ribosomal RNA (rRNA) gene clone library data obtained from

[1]Division of Mucosal Immunology, Department of Microbiology and Immunology, The Institute of Medical Science, The University of Tokyo, Tokyo 108-8639, Japan. [2]Core Research for Evolutional Science and Technology, Japan Science and Technology Agency, Saitama 332-0012, Japan. [3]Microbe Division/Japan Collection of Microorganisms, RIKEN BioResource Center, Tsukuba 305-0074, Japan. [4]Laboratory of Vaccine Materials, National Institute of Biomedical Innovation, Osaka 567-0085, Japan. [5]Division of Mucosal Immunology, International Research and Development Center for Mucosal Vaccines, The Institute of Medical Science, The University of Tokyo, Tokyo 108-8639, Japan. [6]Department of Microbiology and Immunology, Columbia University Medical Center, New York, NY 10032, USA. [7]Nippon Institute for Biological Science, Tokyo 198-0024, Japan. [8]Yakult Central Institute, Tokyo 186-8650, Japan. [9]Division of Innate Immune Regulation, International Research and Development Center for Mucosal Vaccines, The Institute of Medical Science, The University of Tokyo, Tokyo 108-8639, Japan. [10]Department of Mucosal Immunology, School of Medicine, Chiba University, 1-8-1 Inohana, Chuou-ku, Chiba, 260-8670, Japan. [11]Laboratory of Host Defense, WPI Immunology Frontier Research Center, Osaka University, Osaka 565-0871, Japan. [12]Department of Obstetrics and Gynecology, Cellular and Molecular Biology Program, University of Michigan Medical Center, Ann Arbor, MI 48109-5617, USA. [13]Institute of Experimental Immunology, University of Zürich, Winterthurerstrasse 190, Zürich CH-8057, Switzerland. [14]Ludwig Institute for Cancer Research and Université Catholique de Louvain, Brussels B-1200, Belgium. [15]Division of Bacterial Infection, The Institute of Medical Science, The University of Tokyo, Tokyo 108-8639, Japan. [16]Medical Mycology Research Center, Chiba University, Chiba 260-8673, Japan. [17]Benno Laboratory, Innovation Center, RIKEN, Wako, Saitama 351-0198, Japan.

isolated ileal mucus samples from naïve mice (Fig. 2D), we did not detect *B. thetaiotaomicron* in our colony, suggesting that other commensals can induce epithelial fucosylation. To identify which indigenous bacteria are responsible for the induction of F-ECs, we analyzed mucus-associated bacterial populations residing in the mouse duodenum (part 1) and ileum (part 4). In contrast to the predominance of *Lactobacillus* in the duodenum, segmented filamentous bacteria (SFB) predominated in the ileum (Fig. 2D); this is consistent with previous studies (*23*, *24*). SFB are Gram-positive bacteria that preferentially colonize the epithelial surface of the terminal ileum, where they induce T helper 17 (T_H17) cells (*25*, *26*). Similar to their effect on T_H17 cell–inducing microbiota (*27*), vancomycin, ampicillin, and to some extent metronidazole—but not neomycin—extinguished epithelial fucosylation (fig. S1, B and C). Furthermore, consistent with the emergence of SFB, epithelial fucosylation is initiated after weaning (*6*, *28*). To investigate whether SFB have the potential to induce F-ECs, we examined mono-associated gnotobiotic mice and found that F-ECs were induced in SFB but not in *Lactobacillus murinus* mono-associated mice (Fig. 2E). Together, these results suggest that epithelial fucosylation in the terminal ileum is induced by commensal bacteria, including SFB, under physiological conditions.

ILC3 are required for epithelial fucosylation

We next investigated the cellular and molecular mechanisms of F-EC induction. Commensal bacteria, including SFB, induce the proliferation of intraepithelial lymphocytes and immunoglobulin A (IgA)–producing cells and the development of T_H17 cells; they also modulate the function of ILCs (*3*, *4*, *25*–*27*, *29*). To assess whether epithelial fucosylation is induced directly by commensal bacteria or is mediated by mucosal immune cells, we first analyzed the epithelial fucose status of T cell–, B cell–, and Rag-deficient mice. The number of F-ECs was not decreased in T cell– or B cell–deficient mice (fig. S2), indicating that T cells and B cells are dispensable for the induction of epithelial fucosylation. Although SFB induce T_H17 cells (*25*, *26*), T_H17 cells are not required for epithelial fucosylation because IL-6, a critical cytokine for T_H17 cell differentiation in the intestine (*30*), was also not necessary for the induction of F-ECs (fig. S3, A to C). We next analyzed RAR-related orphan receptor–γt (RORγt)–deficient mice, which lack the ILC3 subset, in addition to T_H17 cells (*30*, *31*). RORγt-deficient mice exhibited a marked decrease in the number of F-ECs, accompanied by a decrease in *Fut2* expression in ileal ECs (Fig. 3, A to D). These findings suggest that ILC3 are critical inducers of F-ECs. This was further supported by our observation of few F-ECs in the ileum of Id2-deficient mice, which do not develop any of the ILC subsets (Fig. 3, E to G) (*31*, *32*). Although both RORγt- and Id2-deficient mice lack PPs (*33*, *34*), PPs are not necessary for epithelial fucosylation because PP-null mice, generated by treatment with monoclonal antibody (mAb) to IL-7R during fetal growth, had normal levels of F-ECs (fig. S4). ILC3 in the small intestine are aberrantly expanded in Rag-deficient mice (*35*), and elevated numbers of F-ECs were observed in these mice (Fig. 3, H and I), supporting the notion that F-ECs are induced by ILC3. Because ILC3 express higher levels of CD90, they

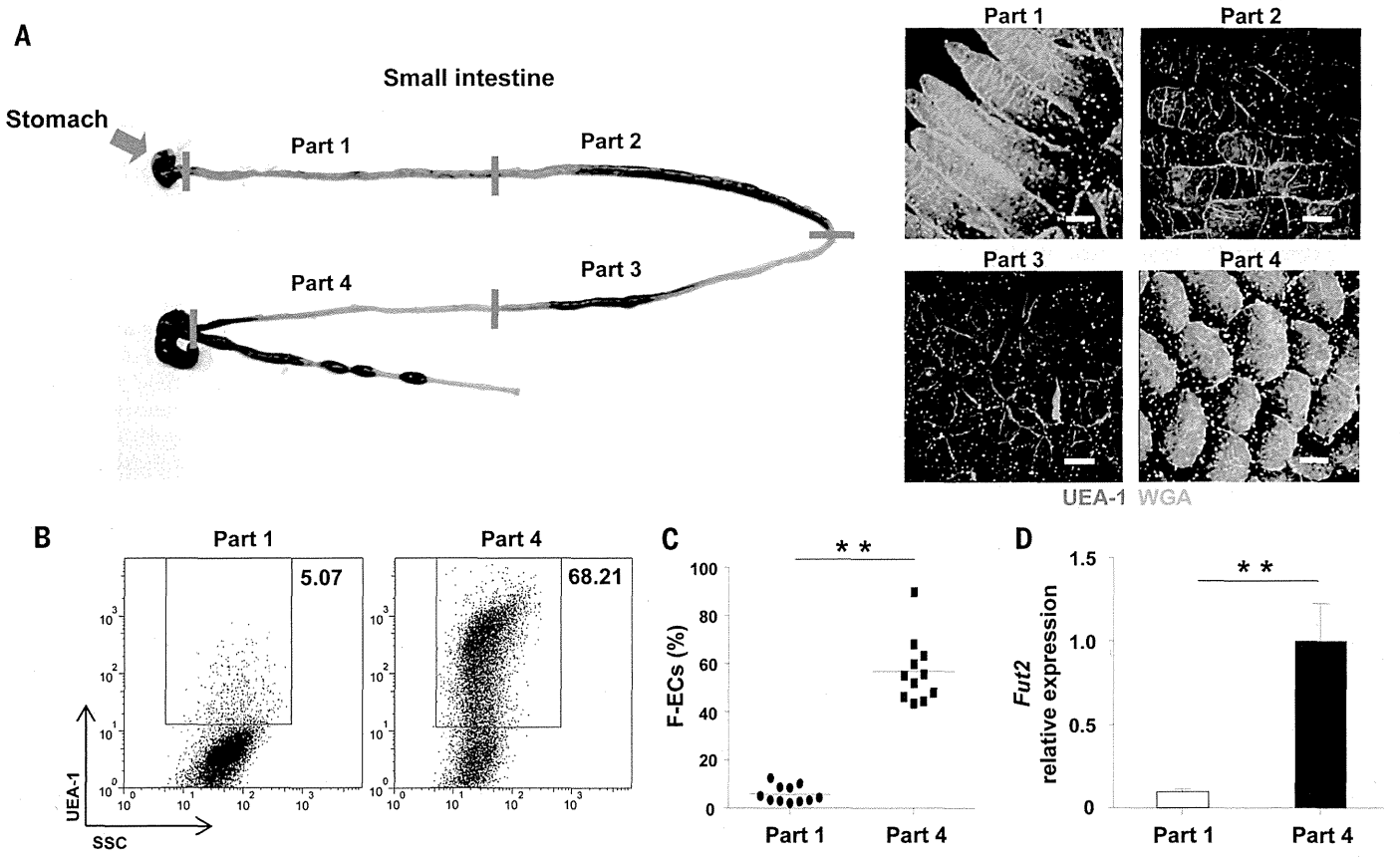

Fig. 1. F-ECs are dominant in the ileum. (**A**) Mouse small intestines were divided equally into 4 parts (parts 1, 2, 3, and 4), from the proximal (duodenum) to the distal (ileum) ends (left), and whole-mount tissues were stained with UEA-1 (red) and WGA (green) to detect F-ECs (UEA-1$^+$ WGA$^+$ cells) (right). Scale bars, 100 μm. Data are representative of three independent experiments. (**B** and **C**) Flow cytometric analysis of intestinal ECs isolated from part 1 and part 4 of the small intestines of C57BL/6 (B6) mice. Representative dot-plots are shown in (B). Percentages and mean numbers (horizontal bars) of fucosylated epithelial cells (n = 11 mice per group) are shown (C). SSC, side scatter. Data of two independent experiments are combined. (**D**) Expression of *Fut2* in ECs isolated from part 1 and part 4 of the small intestine isolated from five to six mice per group. Error bars indicate SD. $^{**}P < 0.01$ by using Student's t test. Data are representative of two independent experiments.

can be depleted with a mAb to CD90 (*36*, *37*). To identify whether ILC3 induce F-ECs, we treated wild-type and Rag-deficient mice with a mAb to CD90. *Fut2* expression and the number of F-ECs were markedly decreased after depletion of ILCs in both wild-type and Rag-deficient mice (Fig. 3, J to M, and fig. S5, A and B). Substantial numbers of SFB were still observed in RORγt-, Id2-, and CD90$^+$ ILC–depleted mice (fig. S6, A and B). Therefore, the defective epithelial fucosylation in these models was not attributable to the absence of F-EC–inducing commensals. Collectively, these results indicate that CD90$^+$ ILC3 are required for the induction and maintenance of F-ECs.

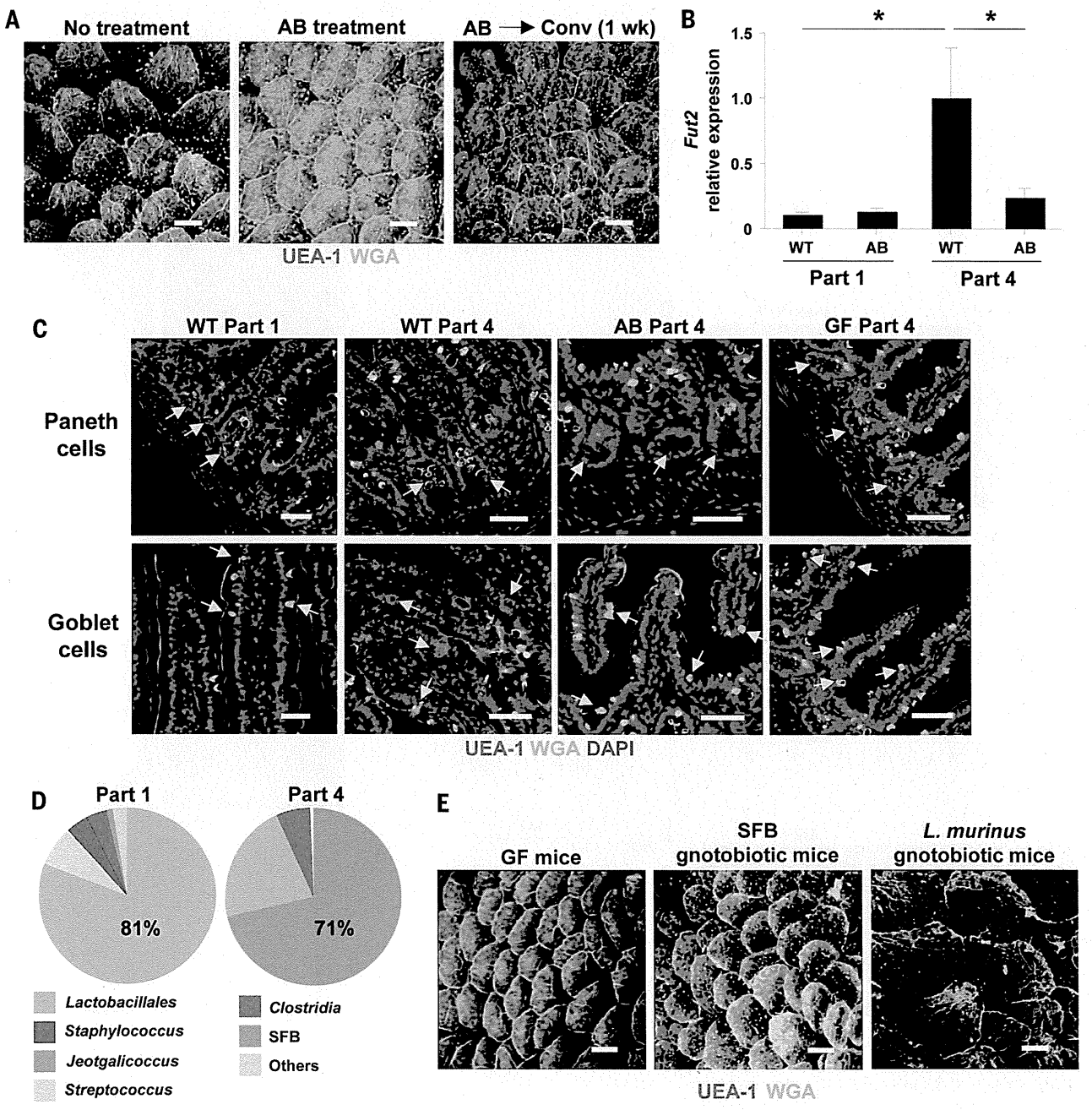

Fig. 2. Commensal bacteria induce epithelial fucosylation under homeostatic conditions. (**A**) Whole-mount ileal tissues of AB-treated mice and conventionalized AB-treated mice were stained with UEA-1 (red) and WGA (green) (n = 3 mice per group). Scale bars, 100 μm. Data are representative of two independent experiments. (**B**) *Fut2* expression in ECs isolated from part 1 (duodenum) and part 4 (ileum) of the small intestines of wild-type (WT) and AB-treated mice (n = 3 mice per group). Error bars indicate SD. *P < 0.05 by using Student's t test. Data are representative of two independent experiments. (**C**) Tissues from part 1 and part 4 of the small intestines of WT, AB-treated, and GF mice were stained with UEA-1 (red), WGA (green), and 4′,6-diamidino-2-phenylindole (DAPI) (blue). Arrows show Paneth cells (top) and goblet cells (bottom). Scale bars, 50 μm. Data are representative of two independent experiments. (**D**) Bacterial populations isolated from the mucus fraction of part 1 and part 4 of mouse small intestine were analyzed by means of 16S rRNA gene clone library. Representative graphs were constructed from samples (part 1, n = 480 clones; Part 4, n = 477 clones) isolated from five different mice (95 or 96 samples were obtained from each mouse). (**E**) Ileal tissues of GF, SFB, or *L. murinus* mono-associated mice (n = 3 mice per group) were stained with UEA-1 (red) and WGA (green). Scale bars, 100 μm. Data are representative of two independent experiments.

IL-22 produced by ILC3 mediates epithelial fucosylation

We next investigated how ILC3 induce epithelial fucosylation. ILC3 cells secrete IL-22, which stimulates the antimicrobial function and maintenance of intestinal ECs (*3*, *4*, *36*, *38*). Indeed, the expression of *Il22* gene was much higher in ILC3 than in any other intestinal immune cell subset (fig. S7A). We therefore assessed whether commensal bacteria regulate ILC3 differentiation and cytokine expression. Although AB-treated or wild-type mice had similar numbers of CD3$^-$ RORγt$^+$

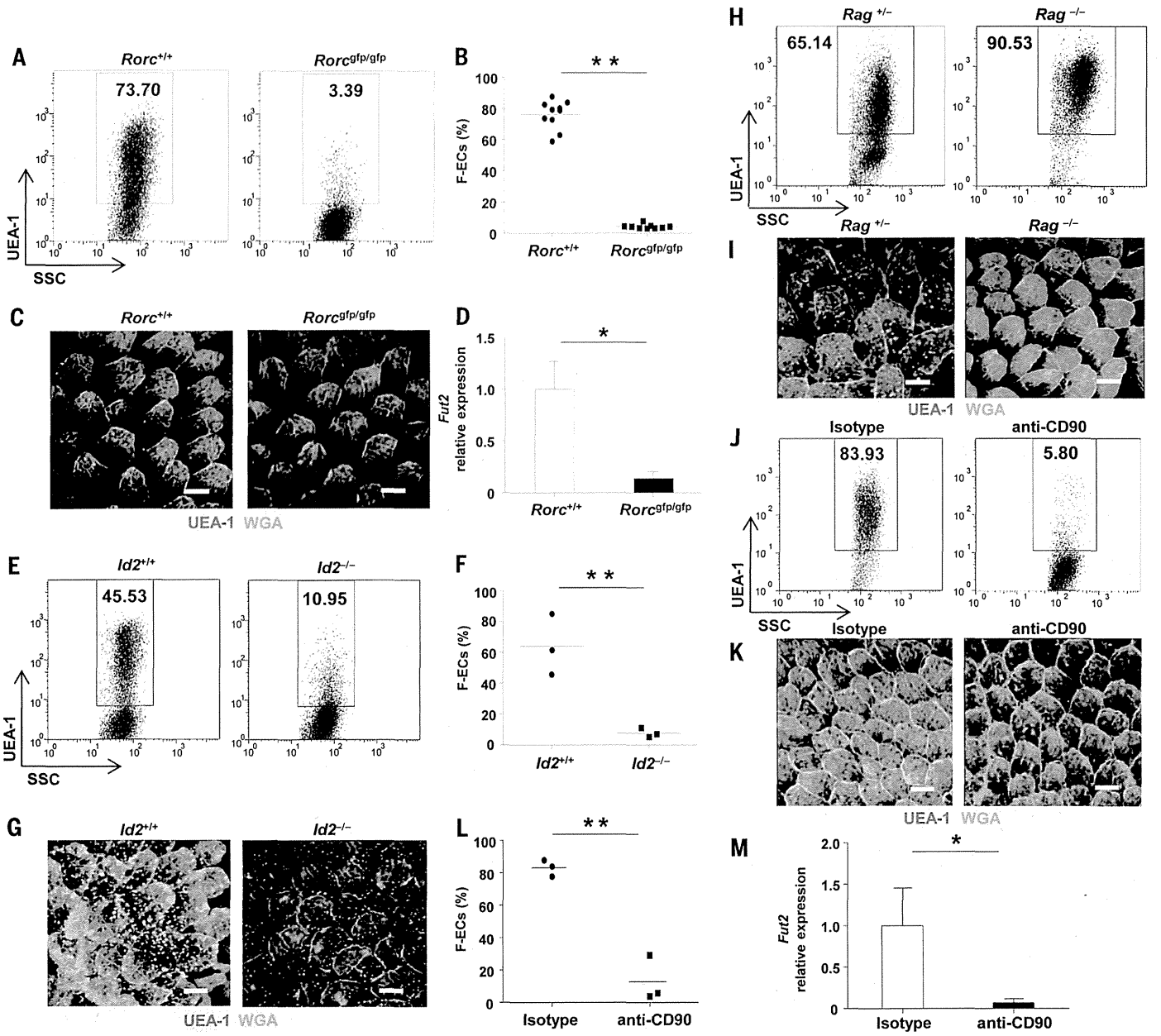

Fig. 3. CD90$^+$ RORγt$^+$ ILC3 induce F-ECs. (**A** and **B**) Representative dot-plots (A) and percentages and means (B) (horizontal bars) of ileal F-ECs isolated from *Rorc*$^{+/+}$ and *Rorc*$^{gfp/gfp}$ mice (n = 10 mice per group). SSC, side scatter. **P < 0.01 by using Student's t test. Data of two independent experiments are combined. (**C**) Whole-mount ileal tissues from *Rorc*$^{+/+}$ and *Rorc*$^{gfp/gfp}$ mice were stained with UEA-1 (red) and WGA (green) (n = 10 mice per group). Scale bars, 100 μm. Data are representative of two independent experiments. (**D**) Expression of *Fut2* in ileal ECs isolated from *Rorc*$^{+/+}$ and *Rorc*$^{gfp/gfp}$ mice (n = 5 mice per group). Data are representative of two independent experiments. Error bars indicate SD. *P < 0.05. (**E** and **F**) Representative dot-plots (E) and percentages and means (F) (horizontal bars) of ileal ECs isolated from *Id2*$^{+/+}$ and *Id2*$^{-/-}$ mice (n = 3 mice per group). Data of three independent experiments are combined. (**G**) Whole-mount staining of ileal villi isolated from *Id2*$^{+/+}$ and *Id2*$^{-/-}$ mice. Scale bars, 100 μm. Data are representative of three independent experiments. (**H** and **J**) Representative dot-plots of ileal ECs isolated from *Rag*$^{+/-}$ and *Rag*$^{-/-}$ mice (H) and *Rag*$^{-/-}$ mice treated with mAb to CD90 (anti-CD90 mAb) or isotype control Ab to CD90 (J) (n = 3 mice per group). (**I** and **K**) Whole-mount staining of ileal villi isolated from *Rag*$^{+/-}$ or *Rag*$^{-/-}$ mice (I) and anti-CD90 mAb– or anti-CD90 isotype control Ab–treated *Rag*$^{-/-}$ mice (K) (n = 3 mice per group). Scale bars, 100 μm. Data are representative of two independent experiments. (**L** and **M**) Percentages and means (horizontal bars) of ileal F-ECs (L) and *Fut2* expression (M) isolated from anti-CD90 mAb– or isotype control Ab–treated *Rag*$^{-/-}$ mice (n = 3 mice per group). Data are representative of two independent experiments. Error bars indicate SD. *P < 0.05, **P < 0.01 by using Student's t test.

ILC3 (fig. S7, B and C), expression of IL-22 was significantly reduced in AB-treated mice but was restored after cessation of AB treatment (fig. S7D). To identify whether IL-22 is involved in the induction of F-ECs, we analyzed mice lacking IL-22 and found that they had reduced numbers of F-ECs; this was correlated with a decrease in epithelial *Fut2* expression (Fig. 4, A and B). We next examined whether IL-22 alone induced epithelial fucosylation. We used hydrodynamic delivery of an *Il22*-encoding plasmid vector so as to ectopically overexpress IL-22 in AB-treated mice (fig. S8, A and B). In both AB-treated wild-type and *Rorc*$^{gfp/gfp}$ mice, F-ECs were induced in both the duodenum (part 1) and the ileum (part 4) in mice ectopically producing IL-22 but not in mice receiving control vector (Fig. 4, C and D, and fig. S8, C and D). This suggests that IL-22 is sufficient for epithelial fucosylation. Expression of *Fut2* was correlated with the presence of IL-22–induced F-ECs (Fig. 4E). To confirm whether IL-22 produced by ILC3 is necessary for epithelial fucosylation, Rag-deficient mice were treated with an antibody in order to neutralize IL-22. Epithelial *Fut2* expression and fucosylation were interrupted by the neutralization of IL-22 (Fig. 4, F to H). Microbial analyses of IL-22–deficient and

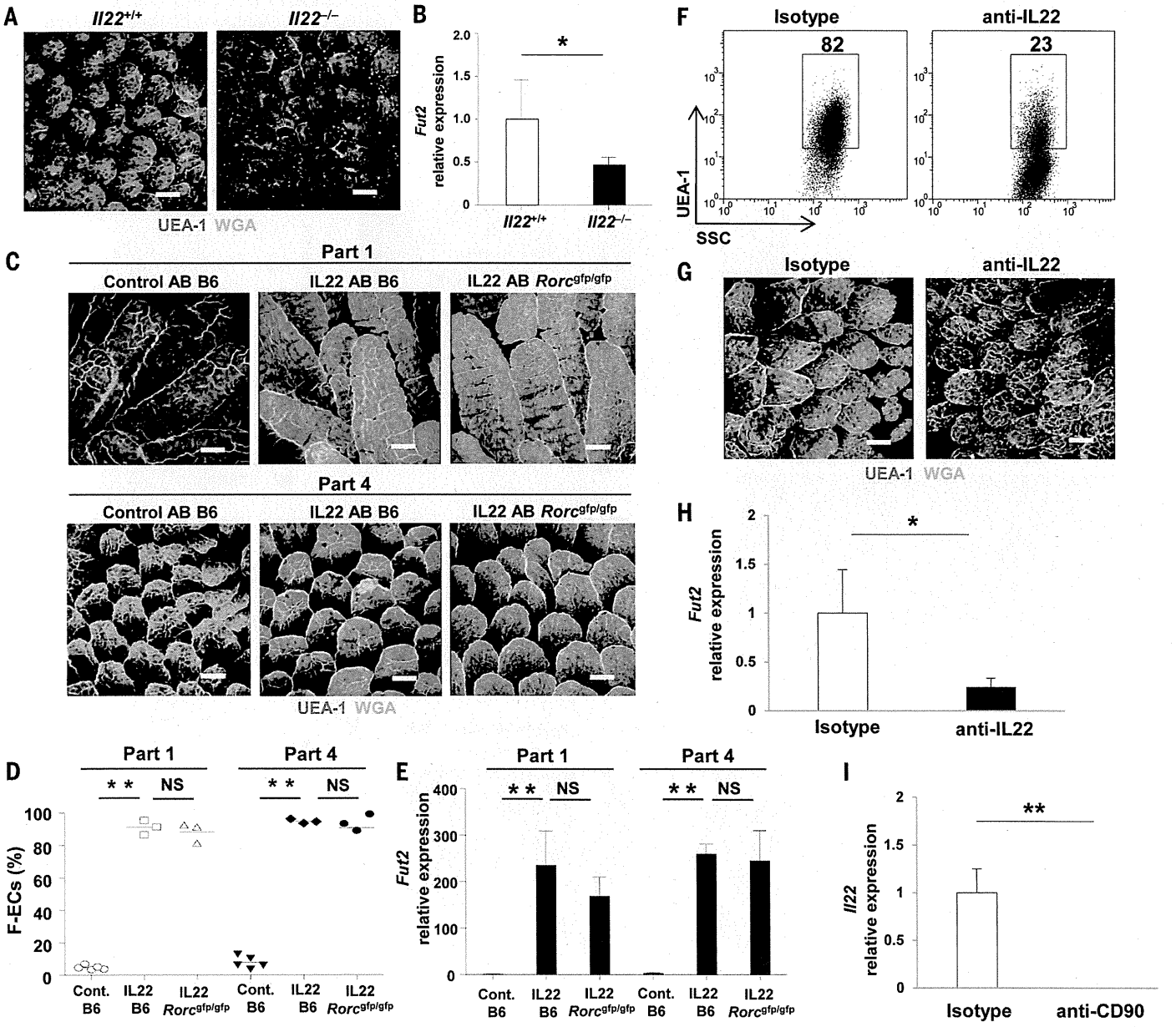

Fig. 4. IL-22 produced by ILCs is involved in the induction of F-ECs. (**A** and **B**) Whole-mount tissues stained with UEA-1 (red) and WGA (green) (A) and gene expression of *Fut2* (B) in ileal villi isolated from *Il22*$^{+/+}$ or *Il22*$^{-/-}$ mice (n = 6 mice per group). Error bars indicate SD. *P < 0.05 by using Student's t test. Scale bars, 100 μm. Data are representative of two independent experiments. (**C** to **E**) AB-treated C57BL/6 (B6) or *Rorc*$^{gfp/gfp}$ mice were intravenously injected with IL-22–encoding plasmid or control vector. Whole-mount staining (C), frequency of F-ECs (D) (mean, horizontal bars), and Fut2 mRNA expression was analyzed by means of rRT-PCR ($n \geq 3$ mice per group) (E). Scale bars, 100 μm. Error bars indicate SD. **P < 0.01 by using Student's t test. NS, not significant. Data are representative of two independent experiments. (**F** to **H**) Representative dot-plots (F), whole-mount histological images (G), and expression of *Fut2* (H) of ileal ECs isolated from *Rag*$^{-/-}$ mice treated with antibody to IL-22 or control Ab. Scale bars, 100 μm. Error bars indicate SD. *P < 0.05 by using Student's t test. (**I**) Expression of *Il22* in ileal LP cells from *Rag*$^{-/-}$ mice treated with antibody to CD90 or control Ab. Error bars inidicate SD. **P < 0.01 by using Student's t test. Data are representative of two independent experiments.

antibody-to-IL-22–treated Rag-deficient mice revealed the presence of SFB (fig. S6, A and B). These findings demonstrate that ILC3-derived IL-22 induced by commensal bacteria mediates epithelial fucosylation. Furthermore, depletion of ILC3 by injecting antibody to CD90 into Rag-deficient mice resulted in marked reduction of IL-22 expression (Fig. 4I), supporting the notion that IL-22–mediated signals produced by ILC3 are a key part of the EC fucosylation cascade. IL-22R is composed of two subunits, IL-22R1 and IL-10Rβ (*39*). Whereas IL-10Rβ was ubiquitously expressed, expression of IL-22R1 was specifically detected in intestinal ECs and was not reduced, even after the depletion of commensal bacteria (fig. S9, A and B). Taken together, our findings indicate that commensal bacteria provide signals that prompt ILC3 to produce IL-22, which leads to the induction of Fut2 by IL-22R–positive intestinal ECs.

LTα expressed by ILC3 induces epithelial fucosylation

ILC3 support the development and maintenance of secondary lymphoid tissues through the expression of lymphotoxins (LTs)—especially LTα1β2 (*40*). The expression of *Lta* and *Ltb* genes was higher in ILC3 than in any other intestinal immune cell subset (fig. S10A). In contrast to IL-22, which was induced by commensal bacteria, *Lta* and *Ltb* gene expression in ILC3 was not affected by commensal flora because the AB treatment did not alter the gene expression (fig. S10B). However, intestinal epithelial fucosylation and *Fut2* expression were severely impaired in $Lta^{-/-}$ mice (Fig. 5, A to C). $Lta^{-/-}$ mice possess congenital defects in secondary lymphoid organs (*41*). To elucidate the contribution of LTα to epithelial fucosylation in adult mice that have established secondary lymphoid organs, wild-type mice were treated with LTβR-Ig, which blocks LTα1β2 signaling. Epithelial fucosylation was attenuated by treatment with LTβR-Ig (Fig. 5, D to E), implying that a continuous LT signal is required for epithelial fucosylation. To investigate whether LTα in ILC3 is crucial for the induction of F-ECs, we constructed mixed bone marrow (BM) chimeric mice by transferring BM cells taken from

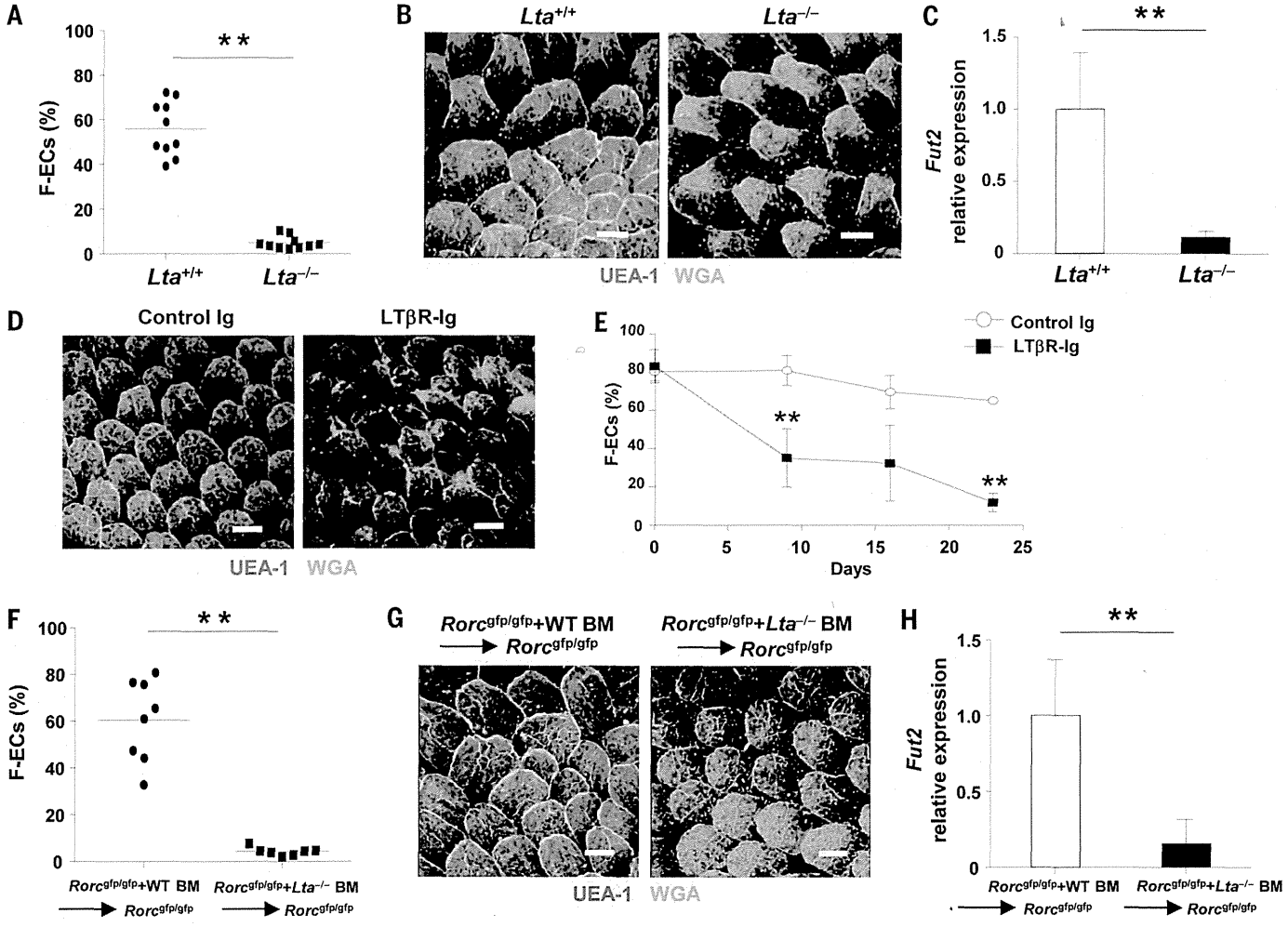

Fig. 5. LTs in innate lymphoid cells induce F-ECs. (**A**) Representative values and means (horizontal bars) of frequency of ileal F-ECs isolated from $Lta^{+/+}$ or $Lta^{-/-}$ mice (n = 10 mice per group). Data of two independent experiments are combined. $^{**}P < 0.01$ by using Student's t test. (**B**) Representative whole-mount staining of ileal villi isolated from $Lta^{+/+}$ or $Lta^{-/-}$ mice (n = 10 mice per group). Scale bars, 100 μm. (**C**) Expression of *Fut2* in ileal ECs isolated from $Lta^{+/+}$ or $Lta^{-/-}$ mice (n = 5 mice per group). Error bars inidicate SD. $^{**}P < 0.01$ by using Student's t test. Data are representative of two independent experiments. (**D**) Representative whole-mount staining of ileal villi from C57BL/6 mice injected with control IgG or LTβR-Ig. Tissues were stained with UEA-1 (red) and WGA (green). (n = 3 mice per group) (**E**) Frequencies of F-ECs in the ileum of C57BL/6 mice injected with control IgG (control Ab) or LTβR-Ig twice (day 9), 3 times (day 16), or 4 times (day 23) (n = 3 mice per group). Error bars indicate SD. $^{**}P < 0.01$ by using Student's t test. (**F** to **H**) Values and means (F), representative whole-mount staining (G), and expression of *Fut2* (H) in ileal ECs isolated from $Rorc^{gfp/gfp}$ mice injected with a mixture of BM cells from $Rorc^{gfp/gfp}$ and WT mice or $Rorc^{gfp/gfp}$ and $Lta^{-/-}$ mice (n = 7 to 8 mice per group). Data of two independent experiments are combined. Error bars indicate SD. $^{**}P < 0.01$ by using Student's t test. Scale bars, 100 μm.

LTα-deficient or -sufficient mice and mixed with BM cells from RORγt-deficient mice into lethally irradiated recipients. F-ECs and *Fut2* expression were diminished in recipient mice reconstituted with BM cells containing LTα-deficient RORγt$^+$ ILC3, whereas substantial numbers of F-ECs, and *Fut2* expression, were induced in recipient mice reconstituted with BM cells containing LTα-sufficient RORγt$^+$ ILC3, indicating the importance of LTα expressed by ILC3 in the induction of F-ECs (Fig. 5, F to H). When the microbiota of LTα-deficient mice or of mixed BM chimeras containing LTα-deficient ILC3 were examined, substantial numbers of SFB were observed (fig. S6, A and B). From these results, we concluded that induction and maintenance of F-ECs were also regulated by ILC3-derived LT in a commensal flora–independent manner.

Epithelial fucosylation protects against infection by *Salmonella typhimurium*

We next investigated the physiological role of epithelial fucosylation. With exception of Paneth cells, the *Fut2* expression and ileal epithelial fucosylation observed in wild-type mice were abolished in *Fut2*$^{-/-}$ mice (fig. S11, A to E). We did not detect any overt changes in mucosal leukocyte populations or in IL-22 or LT expression in ILC3 in these mice (fig. S11F and table S1). Epithelial fucosylation provides an environmental platform for colonization by *Bacteroides* species (*6*–*9*); however, it is unknown whether epithelial fucosylation affects colonization and subsequent infection by pathogenic bacteria. To assess the effects of intestinal fucosylation on pathogenic bacterial infection, we first infected GF mice with the enteropathogenic bacterium *Salmonella typhimurium*, which has the potential to attach to fucose-containing carbohydrate molecules (*42*). After infection with *S. typhimurium*, ECs from both part 1 (duodenum) and part 4 (ileum) of the mouse intestine were fucosylated, and this was correlated with Fut2 expression (Fig. 6, A and B). Previous reports have shown that expression of IL-22 in ILCs is much higher in mice infected with *S. typhimurium* (*43*, *44*). Therefore, *S. typhimurium*–induced epithelial fucosylation may be mediated by ILC3. Indeed, epithelial fucosylation was not induced in RORγt-deficient mice after *S. typhimurium* infection (Fig. 6C). To investigate whether epithelial fucosylation has a role in regulating pathogenic bacterial infection, we infected wild-type or *Fut2*$^{-/-}$ mice with *S. typhimurium* and examined disease progression. Compared with wild-type mice, *Fut2*$^{-/-}$ mice were more susceptible to *Salmonella* infection accompanied with the observation of severe inflamed cecum (Fig. 6D). Consistent with the inflammatory status of diseased mice, the numbers of infiltrating leukocytes in cecum were higher in *Fut2*$^{-/-}$ mice than in wild-type mice (Fig. 6E). Although *S. typhimurium* titers in cecal contents were comparable between wild-type and *Fut2*$^{-/-}$ mice, increased numbers of *S. typhimurium* infiltrated the cecal tissue of *Fut2*$^{-/-}$ mice (Fig. 6F). These results suggest that epithelial fucosylation is dispensable for luminal colonization by *S. typhimurium* but inhibits bacterial invasion of intestinal

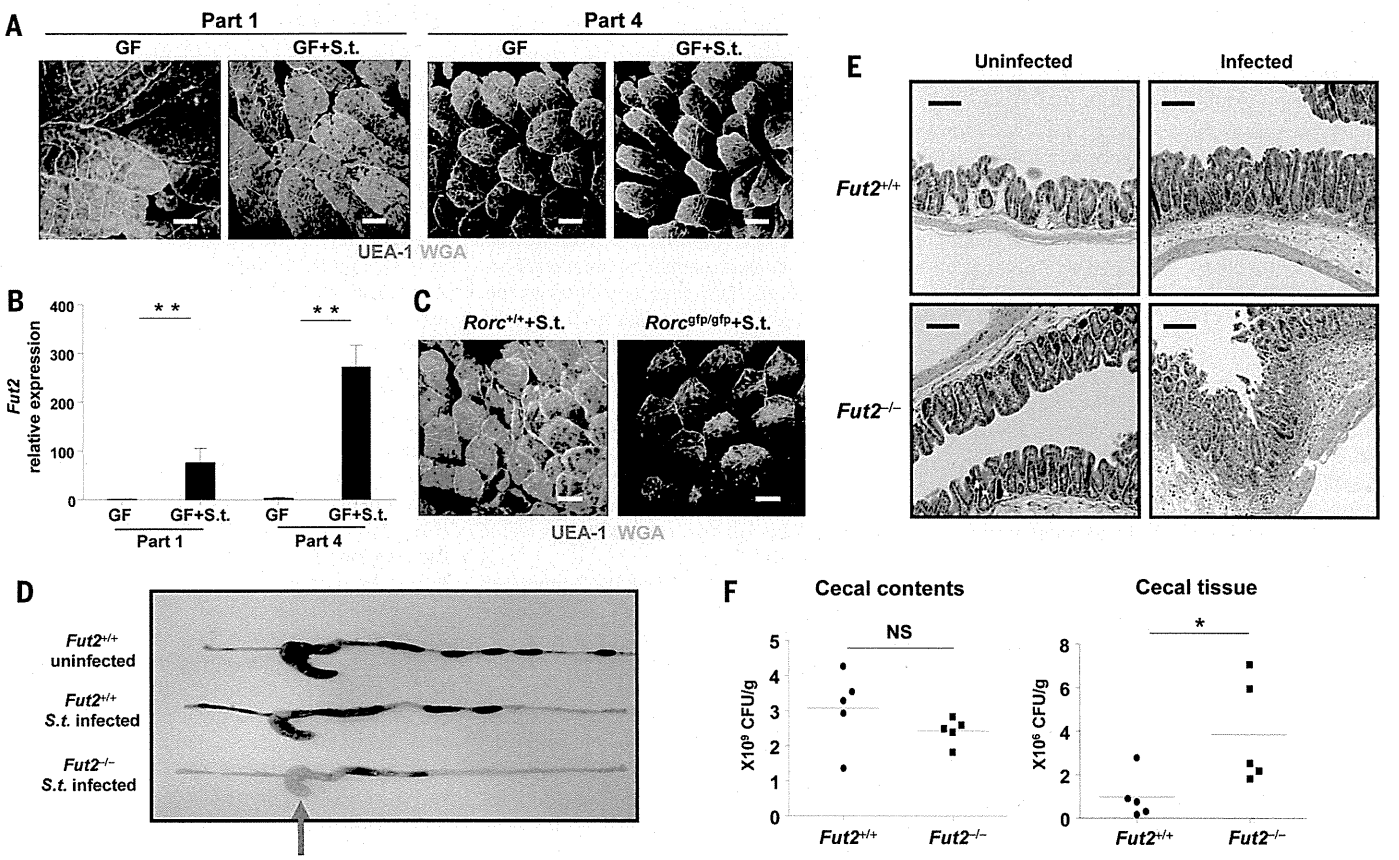

Fig. 6. Epithelial fucosylation protects against infection by *S. typhimurium*. (**A**) Whole-mount tissues from part 1 (duodenum) and part 4 (ileum) of the small intestines of germ-free (GF) or *S. typhimurium*–infected GF mice were stained with UEA-1 (red) and WGA (green) (n = 3 to 4 mice per group). Scale bars, 100 μm. (**B**) Epithelial Fut2 expression in part 1 and part 4 of the small intestines of GF and *S. typhimurium*–infected GF mice was analyzed by using quantitative PCR (n = 3 to 4 mice per group). Error bars indicate SD. $^{**}P < 0.01$ by using Student's t test. (**C**) Whole-mount tissues from ileum of *S. typhimurium*–infected *Rorc*$^{+/+}$ or *Rorc*$^{gfp/gfp}$ mice were isolated and stained with UEA-1 (red) and WGA (green) (n = 3 to 4 mice per group). Scale bars, 100 μm. (**D** and **E**) *Fut2*$^{+/+}$ or *Fut2*$^{-/-}$ mice were infected with *S. typhimurium*. Red arrow shows inflammation of the cecum. Representative macroscopic images (D) and hematoxylin and eosin–stained cecal sections (E) of infected or uninfected mice (n = 5 mice per group). Scale bars, 100 μm. (**F**) Numbers of bacteria in the luminal contents, and within the tissues, of the ceca of *Fut2*$^{+/+}$ or *Fut2*$^{-/-}$ mice were counted 24 hours after infection (n = 5 mice per group). $^{*}P < 0.05$ by using Student's t test. NS, not significant. Three independent experiments were performed with similar results.

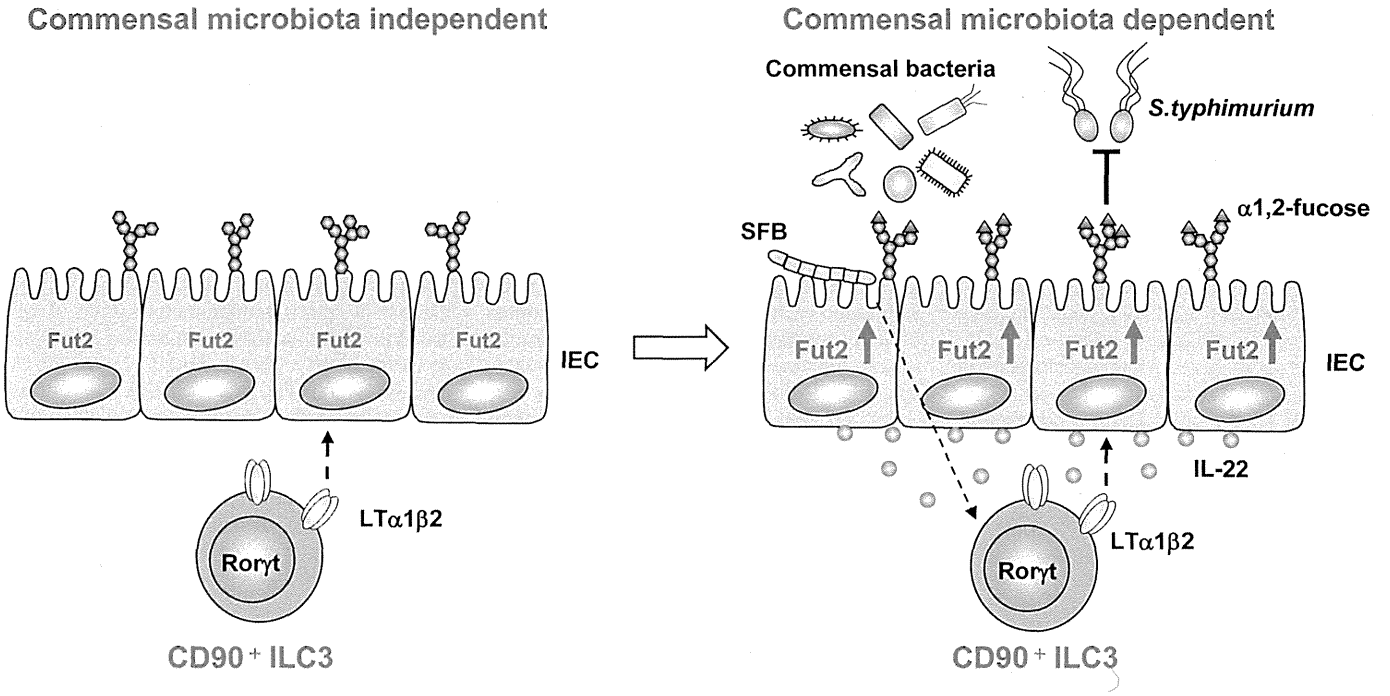

Fig. 7. Scheme for the induction and regulation of epithelial fucosylation by ILC3. IL-22– and LTα-producing ILC3 are critical cells for the induction and regulation of F-ECs. ILC3-mediated fucosylation of ECs is operated by commensal microbiota–dependent and –independent manners. Commensal bacteria, including SFB, stimulate CD90$^+$ ILC3 to produce IL-22 for the induction of Fut2 in ECs. On the other hand, LTα production by ILC3 are operated by a commensal bacteria–independent manner. ILC3-derived IL-22 and LTα induce Fut2 and subsequent epithelial fucosylation, which inhibits infection by *S. typhimurium*. IEC, intestinal epithelial cell.

tissues. Collectively, these results indicate that epithelial fucosylation, regulated by *Fut2*, has a protective role against infection by pathogenic bacteria.

Discussion

The results of recent genome-wide association studies imply that FUT2 nonsense polymorphisms affect the incidence of various metabolic and inflammatory diseases, including chronic intestinal inflammation such as Crohn's disease and infections with pathogenic microorganisms, especially Norwalk virus and rotavirus in humans (*13*–*19*). Understanding the mechanisms of regulation of Fut2 gene expression and fucosylation, one of the major glycosylation events in intestinal ECs, is therefore of great interest. Previously, it was thought that epithelial fucosylation is initiated by direct interaction between commensals and ECs (*7*). Indeed, several reports have shown that epithelial fucosylation is actively induced and used by *Bacteroides* (*8*, *9*). Here, we unexpectedly found that microbiota–epithelia cross-talk is insufficient to induce epithelial fucosylation, and rather, CD90$^+$ RORγt$^+$ ILC3 are necessary for induction of epithelial *Fut2* expression and consequent fucosylation. ILC3 located in the intestinal lamina propria express high levels of IL-22 in a commensal bacteria–dependent manner (Fig. 4I and fig. S7, A and D). This IL-22 then presumably binds to IL-22R expressed by intestinal ECs, leading to the induction of Fut2 and initiation of the EC fucosylation process (Fig. 7). In contrast to the expression of IL-22, ILC3 express LT in a commensal bacteria–independent manner. Spontaneous expression of LT on ILC3 also contributes to the induction of epithelial fucosylation. To explain the mechanism underlying induction of epithelial fucosylation, we propose that epithelial fucosylation is regulated by a two-phase system orchestrated by ILC3 through the microbiota-independent production of LT and the induction of IL-22 by commensal bacteria (Fig. 7). Although other types of stimulation may also affect epithelial fucosylation, our findings reveal a critical role for ILC3.

Our results demonstrated that IL-22 produced by ILC3 is necessary and sufficient for induction of epithelial fucosylation when ILC3 are appropriately stimulated by commensal microbiota (Fig. 4, A to E). In addition to IL-22–mediated epithelial fucosylation, our results also show that the level of epithelial fucosylation is markedly reduced under LTα-deficient conditions (Fig. 5, A to C). Our findings suggest two possibilities for the IL-22/LT-mediated regulation of epithelial fucosylation. The first is that Fut2 expression and subsequent epithelial fucosylation are induced when the intensity of synergistic or additive signals from IL-22 and LT is above the threshold for activation of Fut2. For example, LT produced by ILC3 provides the baseline signal for the minimum expression of Fut2, whereas commensal-mediated IL-22 produced by ILC3 drives the maximum expression of Fut2 for the induction of epithelial fucosylation. The second possibility is that LT directly or indirectly regulates the expression of IL-22R by ECs, and vice versa, and/or the expression of IL-22. Indeed, a previous report has shown that LT produced by ILC3 regulates the expression of IL-23 by intestinal dendritic cells, as well as the subsequent production of IL-22 by ILC3 after infection with *C. rodentium* (*45*). How ILC3-derived IL-22 and LT regulate epithelial Fut2 expression remains to be further elucidated.

Our findings provide further evidence of the critical roles of commensal microbiota, epithelial cells, and innate immune cells (such as ILC3) in the creation of a protective platform against infection by pathogenic bacteria (Fig. 7). Ablation of epithelial fucose allowed severe infection by the pathogenic bacteria *S. typhimurium* (Fig. 6, D to F). Although the detailed mechanisms of why *Fut2*$^{-/-}$ mice are susceptible to *Salmonella* infection remain unknown, one possibility is that fucosylated mucin produced by goblet cells blocks the attachment of *S. typhimurium* to the epithelium. Commensal microbes continuously stimulated goblet cells to release fucosylated mucin into the intestinal lumen (Fig. 2C). Indeed, in a previous in vitro study, H-type 2 antigens, which are synthesized by Fut2 in intestinal ECs, prevented the binding of *S. typhimurium* to fucosylated epithelia; this supports our present findings (*42*). Our findings suggest a protective role for ILC3-mediated mucus-associated fucosylated glycan against infection by pathogenic bacteria.

ILC3 play critical roles in regulation of immune responses during mucosal infection, especially

by producing IL-22, which promotes subsequent expression of the antimicrobial molecule RegIIIγ by ECs (*4*, *36*, *45*). In addition to this, our results describe a previously unknown biological role for ILC3 in the induction and maintenance of intestinal epithelial glycosylation, which leads to the creation of an antipathogenic bacterial platform in the intestine (Fig. 7). Furthermore, epithelial fucosylation contributes to the creation of a cohabitation niche for the establishment of normal commensal microbiota (*20*, *21*). Thus, ILC3-mediated control of epithelial-surface glycosylation might represent a general strategy for regulating the gut microenvironment. Targeted modification of these mechanisms has the potential to provide novel approaches for the control of intestinal infection and inflammation.

Materials and Methods

Mice

C57BL/6 and BALB/c mice were purchased from CLEA Japan (Tokyo, Japan). *Fut2*$^{-/-}$ and *Il22*$^{-/-}$ mice (C57BL/6 background) were generated as described previously, and *Id2*$^{-/-}$ mice were kindly provided by Y. Yokota (*33*, *46*, *47*). *Fut2*$^{-/-}$ mice were crossed onto the BALB/c background for six generations. *Rag2*$^{-/-}$ mice were kindly provided by F. Alt. *Rag1*$^{-/-}$; *Rorc*$^{gfp/gfp}$, *Il6*$^{-/-}$, *Ltα*$^{-/-}$, *Tcrβ*$^{-/-}$*δ*$^{-/-}$, and *Igh6*$^{-/-}$ mice were purchased from The Jackson Laboratory. Antibiotic-treated mice were fed a cocktail of broad-spectrum antibiotics—namely, ampicillin (1 g/L; Sigma, Bandai, Japan), vancomycin (500 mg/L; Shionogi, Osaka, Japan), neomycin (1 g/L; Sigma), and metronidazole (1 g/L; Sigma)—or were given these antibiotics in their drinking water, for 4 weeks as previously described (*48*). These mice were maintained in the experimental animal facility at the University of Tokyo. GF and SFB or *L. murinus* gnotobiotic mice (BALB/c) were maintained in the GF animal facility at the Yakult Central Institute and at the University of Tokyo. In all experiments, littermates were used at 6 to 10 weeks of age.

Isolation of bacterial DNA

The isolation protocol for bacterial DNA was adapted from a previously described method (*49*), with some modifications. Bacterial samples in the duodenum and ileum were obtained from mice aged 8 weeks. After removal of PPs and intestinal contents, the intestinal tissues were washed three times with phosphate-buffered saline (PBS) for 10 s each time so as to collect bacteria embedded within the intestinal mucus for analysis of microbial composition. These bacteria-containing solutions were centrifuged, and the pellets were suspended in 500 μL of TE buffer (10 mM Tris-HCl, 1 mM EDTA; pH 8.0). Glass beads, Tris-phenol buffer, and 10% sodium dodecyl sulfate (SDS) were added to the bacterial suspensions, and the mixtures were vortexed vigorously for 10 s by using a FastPrep FP100 A (BIO 101). After incubation at 65°C for 10 min, the solutions were vortexed and incubated again at 65°C for 10 min. Bacterial DNA was then precipitated in isopropanol, pelleted by centrifugation, washed in 70% ethanol, and resuspended in TE buffer. Extracted bacterial DNA was subjected to 16*S* rRNA gene clone library (*50*).

16S rRNA gene clone library analyses

For 16*S* rRNA gene clone library analyses, bacterial 16*S* rRNA gene sequences were amplified by means of polymerase chain reaction (PCR) with the 27F (5′-AGAGTTTGATCCTGGCTCAG-3′) and 1492R (5′-GGTTACCTTGTTACGACTT-3′) primers. Amplified 16*S* rDNA was ligated into the pCR4.0 TOPO vector (Invitrogen, Carlsbad, CA), and the products of these ligation reactions were then transformed into DH-5α–competent cells (TOYOBO, Osaka, Japan). Inserts were amplified and sequenced on an ABI PRISM 3100 Genetic Analyzer (Applied Biosystems, Foster City, CA). The 27F and 520R (5′-ACCGCGGCTGCTGGC-3′) primers and a BigDye Terminator cycle sequencing kit (Applied Biosystems) were used for sequencing. Bacterial sequences were identified by means of Basic Local Alignment Search Tool (BLAST) and Ribosomal Database Project searches (*50*).

Immunohistochemistry

Immunohistochemical analyses were performed as previously described, with some modifications (*51*). For whole-mount immunofluorescence staining, the mucus layer was removed by flushing the small intestine with PBS; then, the appropriate parts of the small intestine were fixed with 4% paraformaldehyde for 3 hours. After being washing with PBS, whole-mount tissues were stained for at least 3 hours at 4°C with 20 μg/mL UEA-1 conjugated to tetramethylrhodamine B isothiocyanate (UEA-1-TRITC; Vector Laboratories, Burlingame, CA) and 10 μg/mL wheat germ agglutinin (WGA) conjugated to Alexa Fluor 633 (Invitrogen). For whole-mount fluorescence in situ hybridization analysis, we modified the protocol previously described (*52*). After fixation with 4% paraformaldehyde, intestinal tissues were washed with 1 mL PBS and 100 μL hybridization buffer (0.9 M NaCl, 20 mM Tris-HCl, 0.1% SDS) containing 2 μg EUB338 probe (5′-GCTGCCTCCCGTAGGAGT-3′) conjugated to Alexa Fluor 488 (Invitrogen). After overnight incubation at 42°C, the tissues were washed with 1 mL PBS and stained for 3 hours with 10 μg/mL WGA conjugated to Alexa Fluor 633 in PBS. After being washed with PBS, all tissues were analyzed under a confocal laser-scanning microscope (TCS SP2; Leica Microsystems, Wetzlar, Germany).

Cell preparations

A standard protocol was used to prepare intestinal ECs (*53*). Tissues of the small intestine were extensively rinsed with PBS after removal of PPs. After the intestinal contents had been removed, the samples were opened longitudinally and cut into 1-cm pieces. These tissue pieces were mildly shaken in 1 mM EDTA/PBS for 10 min at 37°C. After passage through a 40-μm mesh filter, intestinal ECs were resuspended in minimum essential medium containing 20% fetal calf serum (FCS). Lamina propria (LP) cells were collected as previously described (*54*), with some modifications. Briefly, isolated small intestine was shaken for 40 min at 37°C in RPMI 1640 containing 10% FCS and 1 mM EDTA. Cell suspensions, including intestinal ECs and intraepithelial lymphocytes, were discarded, and the remaining tissues were further digested with continuous stirring for 60 min at 37°C with 2 mg/mL collagenase (Wako) in RPMI 1640 containing 10% FCS. After passage through a 190-μm mesh, the cell suspensions were subjected to Percoll (GE Healthcare) density gradients of 40 and 75%, and the interface between the layers was collected to retrieve LP cells. Stromal cells were identified as CD45$^-$ Viaprobe$^-$ cells. For fluorescence-activated cell-sorting (FACS) analysis of ILCs, isolated LP cells were further purified by magnetic-activated cell sorting so as to eliminate CD11b$^+$, CD11c$^+$, and CD19$^+$ cells. CD11b$^-$ CD11c$^-$ CD19$^-$ Viaprobe$^-$ CD45$^+$ LP cells were used to detect ILCs.

Antibodies and flow cytometry

For flow cytometric analysis, isolated intestinal ECs were stained with UEA-1-TRITC, anti-CD45–Pacific blue (PB; Biolegend, San Diego, CA), and Viaprobe (BD Biosciences, East Rutherford, NJ). Viaprobe$^-$ CD45$^-$ UEA-1$^+$ cells were identified as F-ECs. After blocking with anti-CD16/32 (FcγRII/III) (BD Biosciences), the following antibodies were used to stain spleen and LP cells: anti-CD45–PB (Biolegend), anti-CD11b–phycoerythrin (PE), anti-Foxp3-fluorescein isothiocyanate (FITC) (eBioscience, San Diego, CA), anti-CD11c–allophycocyanin (APC), anti-CD11b–FITC, anti-Gr-1-Alexa647, anti-CD3-APC, anti-B220-PE, anti-B220-APC, anti-IgA-FITC, anti-CD4-eFluor450, anti-CD90.2–FITC, anti-IL-17-PE, and anti-IFNγ-FITC (all from BD Biosciences), and Viaprobe. CD11b$^-$ CD11c$^-$ CD19$^-$ LP cells were purified by using anti-CD11b, anti-CD11c, and anti-CD19 MicroBeads (Miltenyi Biotec, Bergisch Gladbach, Germany). The results were obtained by using a FACSAria cell sorter (BD Biosciences) with FlowJo software (TreeStar, Ashland, Oregon).

Intracellular staining of Foxp3 and cytokines

Isolated LP cells were incubated for 4 hours at 37°C with 50 ng/mL phorbol myristate acetate (Sigma), 500 ng/mL ionomycin (Sigma), and GolgiPlug (BD Bioscience) in RPMI 1640 containing 10% FCS and penicillin and streptomycin. After incubation, cells were stained with antibodies against surface antigens for 30 min at 4°C. The cells were fixed and permeabilized with Cytofix/Cytoperm solution (BD Bioscience), and cytokines were stained with the fluorescence-conjugated cytokine antibodies. A Foxp3 staining buffer set (eBioscience) was used for intracellular staining of Foxp3.

Depletion of CD90$^+$ ILCs

Depletion of CD90$^+$ ILCs was performed as previously described, with some modifications (*36*). Two hundred and fifty micrograms of a mAb to CD90.2 or an isotype control rat IgG2b (BioXCell, West Lebanon, NH) was given by means of intraperitoneal injection a total of three times at

3-day intervals. Intestinal ECs and LP cells were collected 2 days after the final injection.

Hydrodynamic IL-22 gene delivery system

pLIVE control plasmid (Takara Bio, Shiga, Japan) or IL-22–expressing pLIVE vector (pLIVE-*mIl22*) was introduced into 8-week-old antibiotic-treated C57BL/6 or *Rorc*$^{gfp/gfp}$ mice. Ten micrograms per mouse of plasmid diluted in ~1.5 mL TransIT-EE Hydrodynamic Delivery Solution (Mirus Bio, Madison, WI) was injected via the tail vein within 7 to 10 s. To assess IL-22 expression, serum IL-22 was quantified by means of an enzyme-linked immunosorbent assay (R&D Systems, Minneapolis, MN).

Generation of PP-null mice

mAb to IL-7R (A7R34) was kindly provided by S. Nishikawa. PP-null mice were generated by injecting 600 μg of mAb to IL-7R into pregnant mice on embryonic day 14 (*55*).

In vivo treatment with LTβR-Ig and antibody to IL-22

Neutralization antibody to IL-22 was purchased from eBioscience. Eight-week-old Rag-deficient mice were injected intraperitoneally with antibody to IL-22 a total of five times at 3-day intervals (on days 0, 3, 6, 9, and 12). Plasmid pMKIT-expressing LTβR-Ig and LTβR-Ig treatment was performed as described previously (*56*). Four-week-old C57BL/6 mice were injected intraperitoneally once a week for 3 weeks (on days 0, 7, 14, and 21) with LTβR-Ig fusion protein or control human IgG1 at a dose of 50 μg per mouse. Intestinal ECs were analyzed 3 days after the indicated injection time points.

Adoptive transfer of mixed BM

For mixed BM transfer experiments, *Rorc*$^{gfp/gfp}$ mice were irradiated with two doses of 550 rad each, 3 hours apart. BM cells (1×10^7) from *Rorc*$^{gfp/gfp}$ mice was mixed with BM cells (1×10^7) from C57BL/6 or *Ltα*$^{-/-}$ mice and intravenously injected into irradiated recipient mice. BM chimeric mice were used for experiments 8 weeks after the BM transfer.

Isolation of RNA and real-time reverse transcriptase PCR analysis

Intestinal ECs and subsets of LP cells were sorted with a FACSAria cell sorter (BD Biosciences). The sorted cells were lysed in TRIzol reagent (Invitrogen), and total RNA was extracted in accordance with the manufacturer's instructions. RNA was reverse-transcribed by using a SuperScript VILO cDNA Synthesis Kit (Invitrogen). The cDNA was subjected to real-time reverse transcriptase–PCR (rRT-PCR) by using Roche (Basel, Switzerland) universal probe/primer sets specific for *Ltα* (primer F: 5′-tccctcagaagcacttgacc-3′, R: 5′-gagttctgcttgctggggta-3′, probe No. 62), *Ltβ* (primer F: 5′-cctggtgacoctgttgttg-3′, R: 5′-tgctcctgagccaatgatct-3′, probe No. 76), *Il22* (primer F: 5′-tttcctgaccaaactcagca-3′, R: 5′-tctggatgttctggtcgtca-3′, probe No. 17), *Il22r1* (primer F: 5′;-tgctctgttatctgggctacaa-3′, R: 5′-tcaggacacgttggacgtt-3′, probe No. 9), *Il10rβ* (primer F: 5′-attcggagtgggtcaatgtc-3′, R: 5′-gcatctcaggaggtccaatg-3′, probe No. 29), *Fut2* (primer F: 5′-tgtgacttccaccatcatcc-3′, R: 5′-tctgacagggtttggagctt-3′, probe No. 67), and *Gapdh* (primer F: 5′-tgtccgtcgtggatctgac-3′, R: 5′-cctgcttcaccaccttcttg-3′, probe No. 80). RT-PCR analysis was performed with a Lightcycler II instrument (Roche Diagnostics) to measure the expression levels of specific genes.

Infection with S. typhimurium

Streptomycin-resistant wild-type *S. typhimurium* was isolated from *S. typhimurium* strain ATCC 14028. *Fut2*$^{-/-}$ (BALB/c background) and control littermate mice pretreated with 20 mg of streptomycin 24 hours before infection were given 1×10^8 colony-forming units of the isolated *S. typhimurium* via oral gavage. After 24 hours, the mice were dissected, and the cecal contents were collected. Isolated cecum was treated with PBS containing 0.1 mg mL^{-1} gentamicin at 4°C for 30 min so as to kill bacteria on the tissue surface. The cecum was then homogenized and serial dilutions plated in order to determine the number of *S. typhimurium*. Sections of proximal colon were prepared 48 hours after infection. Infiltration of inflammatory cells was confirmed with hematoxylin and eosin staining.

Statistical analysis

Statistical analysis was performed with an unpaired, two-tailed Student's *t*-test. *P* values <0.05 were considered statistically significant.

REFERENCES AND NOTES

1. Y. Goto, I. I. Ivanov, Intestinal epithelial cells as mediators of the commensal-host immune crosstalk. *Immunol. Cell Biol.* **91**, 204–214 (2013). doi: 10.1038/icb.2012.80; pmid: 23318659
2. J. Qiu *et al.*, Group 3 innate lymphoid cells inhibit T-cell-mediated intestinal inflammation through aryl hydrocarbon receptor signaling and regulation of microflora. *Immunity* **39**, 386–399 (2013). doi: 10.1016/j.immuni.2013.08.002; pmid: 23954130
3. S. L. Sanos *et al.*, RORgammat and commensal microflora are required for the differentiation of mucosal interleukin 22-producing NKp46$^+$ cells. *Nat. Immunol.* **10**, 83–91 (2009). doi: 10.1038/ni.1684; pmid: 19029903
4. N. Satoh-Takayama *et al.*, Microbial flora drives interleukin 22 production in intestinal NKp46$^+$ cells that provide innate mucosal immune defense. *Immunity* **29**, 958–970 (2008). doi: 10.1016/j.immuni.2008.11.001; pmid: 19084435
5. S. Vaishnava *et al.*, The antibacterial lectin RegIIIγ promotes the spatial segregation of microbiota and host in the intestine. *Science* **334**, 255–258 (2011). doi: 10.1126/science.1209791; pmid: 21998396
6. L. Bry, P. G. Falk, T. Midtvedt, J. I. Gordon, A model of host-microbial interactions in an open mammalian ecosystem. *Science* **273**, 1380–1383 (1996). doi: 10.1126/science.273.5280.1380; pmid: 8703071
7. L. E. Comstock, D. L. Kasper, Bacterial glycans: Key mediators of diverse host immune responses. *Cell* **126**, 847–850 (2006). doi: 10.1016/j.cell.2006.08.021; pmid: 16959564
8. M. J. Coyne, B. Reinap, M. M. Lee, L. E. Comstock, Human symbionts use a host-like pathway for surface fucosylation. *Science* **307**, 1778–1781 (2005). doi: 10.1126/science.1106469; pmid: 15774760
9. L. V. Hooper, J. Xu, P. G. Falk, T. Midtvedt, J. I. Gordon, A molecular sensor that allows a gut commensal to control its nutrient foundation in a competitive ecosystem. *Proc. Natl. Acad. Sci. U.S.A.* **96**, 9833–9838 (1999). doi: 10.1073/pnas.96.17.9833; pmid: 10449780
10. Y. Goto, H. Kiyono, Epithelial barrier: An interface for the cross-communication between gut flora and immune system. *Immunol. Rev.* **245**, 147–163 (2012). doi: 10.1111/j.1600-065X.2011.01078.x; pmid: 22168418
11. K. Terahara *et al.*, Distinct fucosylation of M cells and epithelial cells by Fut1 and Fut2, respectively, in response to intestinal environmental stress. *Biochem. Biophys. Res. Commun.* **404**, 822–828 (2011). doi: 10.1016/j.bbrc.2010.12.067; pmid: 21172308
12. E. A. Hurd, S. E. Domino, Increased susceptibility of secretor factor gene Fut2-null mice to experimental vaginal candidiasis. *Infect. Immun.* **72**, 4279–4281 (2004). doi: 10.1128/IAI.72.7.4279-4281.2004; pmid: 15213174
13. A. Franke *et al.*, Genome-wide meta-analysis increases to 71 the number of confirmed Crohn's disease susceptibility loci. *Nat. Genet.* **42**, 1118–1125 (2010). doi: 10.1038/ng.717; pmid: 21102463
14. A. Hazra *et al.*, Common variants of FUT2 are associated with plasma vitamin B12 levels. *Nat. Genet.* **40**, 1160–1162 (2008). doi: 10.1038/ng.210; pmid: 18776911
15. L. Lindesmith *et al.*, Human susceptibility and resistance to Norwalk virus infection. *Nat. Med.* **9**, 548–553 (2003). doi: 10.1038/nm860; pmid: 12692541
16. D. P. McGovern *et al.*, International IBD Genetics Consortium, Fucosyltransferase 2 (FUT2) non-secretor status is associated with Crohn's disease. *Hum. Mol. Genet.* **19**, 3468–3476 (2010). doi: 10.1093/hmg/ddq248; pmid: 20570966
17. D. J. Smyth *et al.*, FUT2 nonsecretor status links type 1 diabetes susceptibility and resistance to infection. *Diabetes* **60**, 3081–3084 (2011). doi: 10.2337/db11-0638; pmid: 22025780
18. B. M. Imbert-Marcille *et al.*, A FUT2 gene common polymorphism determines resistance to rotavirus A of the P[8] genotype. *J. Infect. Dis.* **209**, 1227–1230 (2014). doi: 10.1093/infdis/jit655; pmid: 24277741
19. T. Folseraas *et al.*, Extended analysis of a genome-wide association study in primary sclerosing cholangitis detects multiple novel risk loci. *J. Hepatol.* **57**, 366–375 (2012). doi: 10.1016/j.jhep.2012.03.031; pmid: 22521342
20. P. C. Kashyap *et al.*, Genetically dictated change in host mucus carbohydrate landscape exerts a diet-dependent effect on the gut microbiota. *Proc. Natl. Acad. Sci. U.S.A.* **110**, 17059–17064 (2013). doi: 10.1073/pnas.1306070110; pmid: 24062455
21. P. Rausch *et al.*, Colonic mucosa-associated microbiota is influenced by an interaction of Crohn disease and FUT2 (Secretor) genotype. *Proc. Natl. Acad. Sci. U.S.A.* **108**, 19030–19035 (2011). doi: 10.1073/pnas.1106408108; pmid: 22068912
22. R. B. Sartor, Microbial influences in inflammatory bowel diseases. *Gastroenterology* **134**, 577–594 (2008). doi: 10.1053/j.gastro.2007.11.059; pmid: 18242222
23. J. P. Koopman, A. M. Stadhouders, H. M. Kennis, H. De Boer, The attachment of filamentous segmented micro-organisms to the distal ileum wall of the mouse: A scanning and transmission electron microscopy study. *Lab. Anim.* **21**, 48–52 (1987). doi: 10.1258/002367787780740743; pmid: 3560864
24. K. Suzuki *et al.*, Aberrant expansion of segmented filamentous bacteria in IgA-deficient gut. *Proc. Natl. Acad. Sci. U.S.A.* **101**, 1981–1986 (2004). doi: 10.1073/pnas.0307317101; pmid: 14766966
25. V. Gaboriau-Routhiau *et al.*, The key role of segmented filamentous bacteria in the coordinated maturation of gut helper T cell responses. *Immunity* **31**, 677–689 (2009). doi: 10.1016/j.immuni.2009.08.020; pmid: 19833089
26. I. I. Ivanov *et al.*, Induction of intestinal Th17 cells by segmented filamentous bacteria. *Cell* **139**, 485–498 (2009). doi: 10.1016/j.cell.2009.09.033; pmid: 19836068
27. I. I. Ivanov *et al.*, Specific microbiota direct the differentiation of IL-17-producing T-helper cells in the mucosa of the small intestine. *Cell Host Microbe* **4**, 337–349 (2008). doi: 10.1016/j.chom.2008.09.009; pmid: 18854238
28. C. P. Davis, D. C. Savage, Habitat, succession, attachment, and morphology of segmented, filamentous microbes indigenous to the murine gastrointestinal tract. *Infect. Immun.* **10**, 948–956 (1974). pmid: 4426712
29. Y. Umesaki, H. Setoyama, S. Matsumoto, A. Imaoka, K. Itoh, Differential roles of segmented filamentous bacteria and clostridia in development of the intestinal immune system. *Infect. Immun.* **67**, 3504–3511 (1999).pmid: 10377132
30. I. I. Ivanov *et al.*, The orphan nuclear receptor RORγt directs the differentiation program of proinflammatory IL-17$^+$ T helper cells. *Cell* **126**, 1121–1133 (2006). doi: 10.1016/j.cell.2006.07.035; pmid: 16990136
31. H. Spits *et al.*, Innate lymphoid cells—A proposal for uniform nomenclature. *Nat. Rev. Immunol.* **13**, 145–149 (2013). doi: 10.1038/nri3365; pmid: 23348417
32. H. Spits, J. P. Di Santo, The expanding family of innate lymphoid cells: Regulators and effectors of immunity and tissue remodeling. *Nat. Immunol.* **12**, 21–27 (2011). doi: 10.1038/ni.1962; pmid: 21113163

33. Y. Yokota *et al.*, Development of peripheral lymphoid organs and natural killer cells depends on the helix-loop-helix inhibitor Id2. *Nature* **397**, 702–706 (1999). doi: 10.1038/17812; pmid: 10067894
34. G. Eberl *et al.*, An essential function for the nuclear receptor RORγ(t) in the generation of fetal lymphoid tissue inducer cells. *Nat. Immunol.* **5**, 64–73 (2004). doi: 10.1038/ni1022; pmid: 14691482
35. S. Sawa *et al.*, RORγt$^+$ innate lymphoid cells regulate intestinal homeostasis by integrating negative signals from the symbiotic microbiota. *Nat. Immunol.* **12**, 320–326 (2011). doi: 10.1038/ni.2002; pmid: 21336274
36. G. F. Sonnenberg, L. A. Monticelli, M. M. Elloso, L. A. Fouser, D. Artis, CD4(+) lymphoid tissue-inducer cells promote innate immunity in the gut. *Immunity* **34**, 122–134 (2011). doi: 10.1016/j.immuni.2010.12.009; pmid: 21194981
37. S. Buonocore *et al.*, Innate lymphoid cells drive interleukin-23-dependent innate intestinal pathology. *Nature* **464**, 1371–1375 (2010). doi: 10.1038/nature08949; pmid: 20393462
38. G. Pickert *et al.*, STAT3 links IL-22 signaling in intestinal epithelial cells to mucosal wound healing. *J. Exp. Med.* **206**, 1465–1472 (2009). doi: 10.1084/jem.20082683; pmid: 19564350
39. G. F. Sonnenberg, L. A. Fouser, D. Artis, Functional biology of the IL-22-IL-22R pathway in regulating immunity and inflammation at barrier surfaces. *Adv. Immunol.* **107**, 1–29 (2010). doi: 10.1016/B978-0-12-381300-8.00001-0; pmid: 21034969
40. M. Tsuji *et al.*, Requirement for lymphoid tissue-inducer cells in isolated follicle formation and T cell-independent immunoglobulin A generation in the gut. *Immunity* **29**, 261–271 (2008). doi: 10.1016/j.immuni.2008.05.014; pmid: 18656387
41. P. De Togni *et al.*, Abnormal development of peripheral lymphoid organs in mice deficient in lymphotoxin. *Science* **264**, 703–707 (1994). doi: 10.1126/science.8171322; pmid: 8171322
42. D. Chessa, M. G. Winter, M. Jakomin, A. J. Bäumler, *Salmonella enterica* serotype Typhimurium Std fimbriae bind terminal α (1,2)fucose residues in the cecal mucosa. *Mol. Microbiol.* **71**, 864–875 (2009). doi: 10.1111/j.1365-2958.2008.06566.x; pmid: 19183274
43. M. Awoniyi, S. I. Miller, C. B. Wilson, A. M. Hajjar, K. D. Smith, Homeostatic regulation of *Salmonella*-induced mucosal inflammation and injury by IL-23. *PLOS One* **7**, e37311 (2012). doi: 10.1371/journal.pone.0037311; pmid: 22624013
44. I. Godinez *et al.*, T cells help to amplify inflammatory responses induced by *Salmonella enterica* serotype Typhimurium in the intestinal mucosa. *Infect. Immun.* **76**, 2008–2017 (2008). doi: 10.1128/IAI.01691-07; pmid: 18347048
45. A. V. Tumanov *et al.*, Lymphotoxin controls the IL-22 protection pathway in gut innate lymphoid cells during mucosal pathogen challenge. *Cell Host Microbe* **10**, 44–53 (2011). doi: 10.1016/j.chom.2011.06.002; pmid: 21767811
46. S. E. Domino, L. Zhang, P. J. Gillespie, T. L. Saunders, J. B. Lowe, Deficiency of reproductive tract α(1,2)fucosylated glycans and normal fertility in mice with targeted deletions of the FUT1 or FUT2 α(1,2)fucosyltransferase locus. *Mol. Cell. Biol.* **21**, 8336–8345 (2001). doi: 10.1128/MCB.21.24.8336-8345.2001; pmid: 11713270
47. K. Kreymborg *et al.*, IL-22 is expressed by Th17 cells in an IL-23-dependent fashion, but not required for the development of autoimmune encephalomyelitis. *J. Immunol.* **179**, 8098–8104 (2007). doi: 10.4049/jimmunol.179.12.8098; pmid: 18056351
48. S. Rakoff-Nahoum, J. Paglino, F. Eslami-Varzaneh, S. Edberg, R. Medzhitov, Recognition of commensal microflora by toll-like receptors is required for intestinal homeostasis. *Cell* **118**, 229–241 (2004). doi: 10.1016/j.cell.2004.07.002; pmid: 15260992
49. T. Matsuki *et al.*, Quantitative PCR with 16S rRNA-gene-targeted species-specific primers for analysis of human intestinal bifidobacteria. *Appl. Environ. Microbiol.* **70**, 167–173 (2004). doi: 10.1128/AEM.70.1.167-173.2004; pmid: 14711639
50. R. Kibe, M. Sakamoto, H. Hayashi, H. Yokota, Y. Benno, Maturation of the murine cecal microbiota as revealed by terminal restriction fragment length polymorphism and 16S rRNA gene clone libraries. *FEMS Microbiol. Lett.* **235**, 139–146 (2004). doi: 10.1111/j.1574-6968.2004.tb09578.x; pmid: 15158273
51. M. H. Jang *et al.*, Intestinal villous M cells: An antigen entry site in the mucosal epithelium. *Proc. Natl. Acad. Sci. U.S.A.* **101**, 6110–6115 (2004). doi: 10.1073/pnas.0400969101; pmid: 15071180
52. T. Obata *et al.*, Indigenous opportunistic bacteria inhabit mammalian gut-associated lymphoid tissues and share a mucosal antibody-mediated symbiosis. *Proc. Natl. Acad. Sci. U.S.A.* **107**, 7419–7424 (2010). doi: 10.1073/pnas.1001061107; pmid: 20360558
53. M. Yamamoto, K. Fujihashi, K. Kawabata, J. R. McGhee, H. Kiyono, A mucosal intranet: Intestinal epithelial cells down-regulate intraepithelial, but not peripheral, T lymphocytes. *J. Immunol.* **160**, 2188–2196 (1998). ; pmid: 9498757
54. N. Ohta *et al.*, IL-15-dependent activation-induced cell death-resistant Th1 type CD8 α β$^+$NK1.1$^+$ T cells for the development of small intestinal inflammation. *J. Immunol.* **169**, 460–468 (2002). doi: 10.4049/jimmunol.169.1.460; pmid: 12077277
55. H. Yoshida *et al.*, IL-7 receptor α$^+$ CD3(-) cells in the embryonic intestine induces the organizing center of Peyer's patches. *Int. Immunol.* **11**, 643–655 (1999). doi: 10.1093/intimm/11.5.643; pmid: 10330270
56. M. Yamamoto *et al.*, Role of gut-associated lymphoreticular tissues in antigen-specific intestinal IgA immunity. *J. Immunol.* **173**, 762–769 (2004). doi: 10.4049/jimmunol.173.2.762; pmid: 15240662

ACKNOWLEDGMENTS

We thank M. Shimaoka, G. Eberl, M. Pasparakis, K. Honda, C. A. Hunter, C. O. Elson, and J. R. Mora for their critical and helpful comments and advice on this research. Y. Yokota and M. Yamamoto kindly provided Id2-deficient mice and LTβR-Ig, respectively. R. Curtis III and H. Matsui kindly provided several strains of *Salmonella typhimurium*. We thank Y. Akiyama for her technical support with the *S. typhimurium* infection model. S. Tanaka gave us helpful technical suggestions for performing flow cytometric analysis. The data presented in this paper are tabulated in the main paper and in the supplementary materials. Sequences of the bacterial 16*S* rRNA genes obtained from duodenal and ileal mucus bacteria have been deposited in the International Nucleotide Sequence Database (accession nos. AB470733 to AB470815). This work was supported by grants from the following sources: the Core Research for Evolutional Science and Technology Program of the Japan Science and Technology Agency (to H.K.); a Grant-in-Aid for Scientific Research on Priority Areas, Scientific Research (S) (to H.K.); Specially Promoted Research (230000-12 to C.S.); Scientific Research (B) (to J.K.); for the Leading-edge Research Infrastructure Program and the Young Researcher Overseas Visits Program for Vitalizing Brain Circulation (to Y.G., J.K., and H.K.); for the Leading-edge Research Infrastructure Program (to J.K. and H.K.) from the Ministry of Education, Culture, Sports, Science and Technology of Japan; the Global Center of Excellence (COE) Program "Center of Education and Research for Advanced Genome-based Medicine" (to H.K.); the Ministry of Health, Labor and Welfare of Japan (to J.K. and H.K.); the Science and Technology Research Promotion Program for Agriculture, Forestry, Fisheries and Food Industry (to J.K.); Mochida Memorial Foundation for Medical and Pharmaceutical Research (to J.K.); the National Institutes of Health (1R01DK098378 to I.I.); and by the Crohn's and Colitis Foundation of America (SRA#259540 to I.I.). The authors declare no conflicts of interest.

SUPPLEMENTARY MATERIALS

www.sciencemag.org/content/345/6202/1254009/suppl/DC1
Figs. S1 to S11
Table S1

27 March 2014; accepted 25 July 2014
10.1126/science.1254009

JVI
Journals.ASM.org

Vaginal Memory T Cells Induced by Intranasal Vaccination Are Critical for Protective T Cell Recruitment and Prevention of Genital HSV-2 Disease

Ayuko Sato,[a] Aldina Suwanto,[a,b] Manami Okabe,[a] Shintaro Sato,[a,g,i] Tomonori Nochi,[c] Takahiko Imai,[d,e,f] Naoto Koyanagi,[d,e] Jun Kunisawa,[a,g,h] Yasushi Kawaguchi,[d,e] Hiroshi Kiyono[a,b,g,i]

Division of Mucosal Immunology, Department of Microbiology and Immunology, Institute of Medical Science, University of Tokyo, Tokyo, Japan[a]; Department of Medical Genome Science, Graduate School of Frontier Science, University of Tokyo, Kashiwa, Chiba, Japan[b]; Graduate School of Agricultural Science, Tohoku University, Sendai, Miyagi, Japan[c]; Division of Molecular Virology, Department of Microbiology and Immunology, Institute of Medical Science, University of Tokyo, Tokyo, Japan[d]; Division of Viral Infection, Department of Infectious Disease Control, International Research Center for Infectious Diseases, Institute of Medical Science, University of Tokyo, Tokyo, Japan[e]; Nippon Institute for Biological Science, Ome, Tokyo, Japan[f]; International Research and Development Center for Mucosal Vaccines, Institute of Medical Science, University of Tokyo, Tokyo, Japan[g]; Laboratory of Vaccine Materials, National Institute of Biomedical Innovation, Ibaraki, Osaka, Japan[h]; Core Research for Evolutional Science and Technology, Japan Science and Technology Agency, Saitama, Japan[i]

ABSTRACT

Protective immunity against genital pathogens causing chronic infections, such as herpes simplex virus 2 (HSV-2) or human immunodeficiency virus, requires the induction of cell-mediated immune responses locally in the genital tract. Intranasal immunization with a thymidine kinase-deficient (TK^-) mutant of HSV-2 effectively induces HSV-2-specific gamma interferon (IFN-γ)-secreting memory T cell production and protective immunity against intravaginal challenge with wild-type HSV-2. However, the precise mechanism by which intranasal immunization induces protective immunity in the distant genital mucosa more effectively than does systemic immunization is unknown. Here, we showed that intranasal immunization with live HSV-2 TK^- induced the production of effector T cells and their migration to, and retention in, the vaginal mucosa, whereas systemic vaccination barely established a local effector T cell pool, even when it induced the production of circulating memory T cells in the systemic compartment. The long-lasting HSV-2-specific local effector T cells induced by intranasal vaccination provided superior protection against intravaginal wild-type HSV-2 challenge by starting viral clearance at the entry site earlier than with intraperitoneal immunization. Intranasal immunization is an effective strategy for eliciting high levels of cell-mediated protection of the genital tract by providing long-lasting antigen (Ag)-specific local effector T cells without introducing topical infection or inflammation.

IMPORTANCE

Intranasal (i.n.) vaccines against sexually transmitted diseases that are caused by viruses such as herpes simplex virus 2 (HSV-2) have long been in development, but no vaccine candidate is currently available. Understanding the cellular mechanisms of immune responses in a distant vaginal mucosa induced by i.n. immunization with HSV-2 will contribute to designing such a vaccine. Our study demonstrated that i.n. immunization with an attenuated strain of HSV-2 generated long-lasting IFN-γ-secreting T cells in vaginal mucosa more effectively than systemic immunization. We found that these vaginal effector memory T cells are critical for the early stage of viral clearance at natural infection sites and prevent severe vaginal inflammation and herpes encephalitis.

Genital herpes, one of the most common sexually transmitted diseases (STDs), causes primary infection in the genital epithelium and establishes lifelong latency in the sacral ganglia (1). In attempts to elicit protective immunity within the genital tract, several vaccine candidates have been tested on humans and experimental animals by using systemic and mucosal immunization routes (2–8). However, a licensed vaccine for genital herpes has not been developed, even though these experimental vaccines induce antigen (Ag)-specific antibody (Ab) responses and cellular immunity systemically in the host (2–8). The immunological mechanisms responsible for protection against primary and secondary herpes simplex virus 2 (HSV-2) challenge require robust CD4 and CD8 T cell responses (9, 10). Induction of Ag-specific effector T cell production in the genital mucosa is the key to developing protective immunity against genital virus infection, because robust systemic memory T cell responses are not necessarily correlated with host protection (11, 12). However, unlike the case with the spleen or liver, for peripheral tissues, such as the vagina, skin, and intestines, infection or inflammation must occur at a local site in order for circulating memory T cells to migrate into the tissue (13–15). Recently, a novel strategy for vaccination against genital herpes infection was developed through the injection of chemokines into the vaginas of mice immunized systemically with an attenuated strain of HSV-2 that lacks thymidine ki-

Received 7 August 2014 Accepted 10 September 2014
Published ahead of print 17 September 2014
Editor: K. Frueh
Address correspondence to Hiroshi Kiyono, kiyono@ims.u-tokyo.ac.jp.
A. Sato and A. Suwanto contributed equally to this work.

doi:10.1128/JVI.02279-14

nase (HSV-2 TK$^-$) to guide the generated circulating memory T cells into the vaginal mucosa (12). As shown by these results, induction of Ag-specific effector T cells and their retention at the potential virus invasion site (e.g., reproductive tissue) is critical for protection against genital virus infection and is key to the design of vaccines for STDs.

Intranasal (i.n.) immunization is an effective vaccine strategy against STDs, such as human immunodeficiency virus and HSV, because it can effectively induce Ag-specific immune responses in the distant vaginal mucosa (16, 17). For instance, Ag-specific Ab responses and protective immunity in the vaginal mucosa are induced more effectively by i.n. immunization than by systemic immunization (5, 6). Previous results have shown that i.n. immunization with HSV-2 TK$^-$ induces the production of HSV-2-specific gamma interferon (IFN-γ)-secreting cells in both the vaginal tract and the draining lymph nodes (dLNs). Subsequent intravaginal (IVAG) wild-type (WT) HSV-2 challenge then induces protective immunity in the genital tract and sensory ganglia at levels comparable to those from IVAG immunization with the same attenuated virus (17). However, the precise cellular mechanisms by which i.n. immunization provides protection against genital herpesvirus infection that is superior to that provided by systemic immunization remain unknown.

Here, we show the advantages of i.n. immunization with live HSV-2 TK$^-$ in generating a pool of long-lasting HSV-2-specific IFN-γ-secreting effector T cells in the female genital tract; this response controls virus proliferation at the entry site and is thus critical for the rapid induction of protective immunity against IVAG challenge with WT HSV-2.

MATERIALS AND METHODS

Mice. Female C57BL/6 mice (age, 6 to 7 weeks) and C57BL/6-Ly5.1 congenic mice (age, 6 to 7 weeks) were purchased from SLC and the Jackson Laboratory, respectively. All of the mice were housed with *ad libitum* food and water on a standard 12-h–12-h light-dark cycle.

Viruses. The virulent HSV-2 strain 186syn$^+$ (WT HSV-2) (18) and its thymidine kinase mutant, 186TKΔKpn (HSV-2 TK$^-$) (19), were gifts from D. Knipe (Harvard Medical School, Boston, MA). HSV-2 was propagated on Vero cells, and its titer was determined as previously described (20).

Ethics statement. All animal experiments were performed in accordance with the Science Council of Japan's Guidelines for Proper Conduct of Animal Experiments. The protocol was approved by the Institutional Animal Care and Use Committee (IACUC) of the Institute of Medical Science, University of Tokyo (IACUC protocol approval numbers PA13-48 and PA11-91).

Immunization and viral challenge. Female mice were immunized with a single i.n. or intraperitoneal (i.p.) dose of live HSV-2 TK$^-$ at 10^5 PFU. For i.n. immunization, anesthetized mice were inoculated by instillation of 5 μl of virus suspension into each nostril. Vaginal challenge was performed with 5×10^4 PFU (83 times the 50% lethal dose [LD_{50}]) of HSV-2 186syn$^+$ at 3 weeks postimmunization (p.i.) by using a previously described protocol (21). Briefly, the mice received a subcutaneous injection of 2 mg medroxyprogesterone acetate (Depo Provera; GE Healthcare) a week before challenge. They were then preswabbed with a sterile calcium alginate swab and inoculated with 10 μl of virus suspension into the vaginal lumen by micropipette. To suppress circulating memory T cell migration into the vagina, 0.5 μg of pertussis toxin (PTx) (Sigma) was injected i.p. at the time points indicated in the figure legends. Disease severity was scored as follows (5): 0, no signs; 1, slight genital erythema and edema; 2, moderate genital inflammation; 3, purulent genital lesions; 4, hind-limb paralysis; and 5, moribund.

Viral titers in vaginal and nasal washes. Vaginal washes were collected on days 1 to 5 after infection by swabbing with calcium alginate swabs and then washing twice with 100 μl of sterile phosphate-buffered saline (PBS). Nasal washes were collected by flushing with 100 μl sterile PBS twice through the posterior choanae (22). Viral titers were obtained by titration of vaginal-wash samples on a Vero cell monolayer, as described previously (20).

Tissue staining. To analyze inflammation in the vaginal tissues, frozen sections of vaginal tissue were stained with hematoxylin and eosin. To analyze the localization of CD4$^+$ T cells, sections were stained with purified anti-CD4 or anti-CD45.1 Ab (eBioscience), or both, followed by biotinylated secondary Abs (Jackson Immuno Research), streptavidin-horseradish peroxidase (Zymed), tyramide-Cy3, or tyramide-fluorescein isothiocyanate (FITC) (PerkinElmer Life and Analytical Sciences), or all of the above, as described in the instructions of the Tyramide Signal Amplification (TSA) system (PerkinElmer Life and Analytical Sciences). For analysis of proliferating cells, purified anti-Ki-67 Abs (eBioscience) were used. All sections were finally counterstained with 4,6-diamidino-2-phenylindole (Sigma) and analyzed under a confocal laser scanning microscope (TCS SP2; Leica).

PCR analysis. By using a DNeasy blood and tissue kit (Qiagen), total DNA was prepared from samples taken at various time points p.i. from the cervical lymph nodes (cLNs) and nasal passages of i.n.-immunized mice. Cells were isolated from the nasal passages (23) and dorsal root ganglion (24) as previously described. PCR amplification was performed with HSV-2 glycoprotein B (gB) gene-specific primers (5′-CTGGTCAGCTTT CGGTACGA-3′ and 5′-CAGGTCGTGCAGCTGGTTGC-3′) to detect HSV-2 viral DNA (20). The reactions were amplified for 40 cycles. To normalize the tissue contents for each sample, a housekeeping gene, *glyceraldehyde 3-phosphate dehydrogenase* (*Gapdh*), was detected by PCR amplification using the primers 5′-TGAACGGGAAGCTCACTGG-3′ and 5′-TCCACCACCCTGTTGCTGTA-3′). To confirm the sensitivity of the PCR analysis with gB-specific primers, PCR was performed with serially diluted HSV-2 gB DNA cloned inside the pET 20b vector (Novagen).

***In vitro* coculture.** To determine the presence of effector T cells, 10^5 CD4 T cells purified with magnetic beads conjugated to anti-CD4 Ab (Miltenyi Biotec) or whole lymphocytes prepared by tissue digestion with collagenase were stimulated for 72 h *in vitro* with irradiated syngeneic splenocytes as antigen-presenting cells in the presence of heat-inactivated virus Ags, as described previously (20). To determine the ability of dendritic cells (DCs) to stimulate HSV-2-specific T cells, 10^5 CD4 T cells from the dLNs of mice immunized i.n. 7 days previously with HSV-2 TK$^-$ were cocultured as described previously (20) with 5×10^4 DCs purified with magnetic beads conjugated to anti-CD11c Ab (Miltenyi Biotec); coculture was performed for 72 h *in vitro* in the absence of added Ags. Culture supernatants or stimulated cells were analyzed for IFN-γ production by enzyme-linked immunosorbent assay (ELISA) or enzyme-linked immunospot (ELISPOT) assay in accordance with the manufacturer's instructions (eBioscience). For analysis of the ELISPOT assay data, the numbers of IFN-γ-secreting cells per vagina or spleen were calculated by subtracting the number of IFN-γ-secreting cells in wells in the absence of Ag from that in wells stimulated with HSV-2 Ags. To determine the percentages of proliferating cells, we performed a bromodeoxyuridine (BrdU) incorporation assay using a BrdU Flow Kit (BD Pharmingen) in accordance with the manufacturer's instructions. Briefly, mice were i.p. injected with 200 μl of 10 mg/ml of BrdU solution (2 mg/mouse) 24 h before challenge. At 24 h postchallenge (p.c.), cells were prepared from the vaginal tissues as described previously (25). The cells were stained with allophycocyanin (APC)-conjugated anti-CD4 Ab (eBioscience), fixed, and then permeabilized for subsequent BrdU staining with FITC-conjugated anti-BrdU Ab.

Adoptive-transfer experiment. CD4 T cells (10^7) from dLNs of congenic mice (Ly5.1) that had been immunized i.n. with HSV-2 TK$^-$ 7 days previously were purified by using magnetically activated cell separation (MACS) beads (MACS MicroBeads; Miltenyi Biotec) (25). The purified cells were then adoptively transferred into C57BL/6 mice (Ly5.2) via the

tail vein (25). Two hours later, the mice were infected IVAG with WT HSV-2. Vaginal tissues 3 days after infection were stained for CD4 (red), CD45.1 (donor-derived cells; green), and nuclei (blue).

For the virus challenge experiments, naïve medroxyprogesterone acetate-injected C57BL/6 mice received 2×10^7 whole cells or 2×10^6 CD4 T cells isolated (by the use of magnetic beads conjugated to anti-CD4 Ab) from the cLNs of C57BL/6 mice that had been immunized i.n. with HSV-2 TK^- 4 days previously. These mice were challenged IVAG with 10^3 PFU (1.6 LD_{50}) of WT HSV-2 4 days after the adoptive transfer.

Data analysis. Data are expressed as means ± standard deviations (SD). Statistical analysis for most comparisons among groups was performed with a two-tailed Student *t* test; differences were considered statistically significant when the *P* value was <0.05.

RESULTS

Intranasal immunization, but not systemic immunization, with a live-attenuated strain of HSV-2 induces early and full protective immunity against IVAG WT HSV-2 infection. As previously reported (17, 26), mice immunized i.n. with HSV-2 TK^- survived without serious genital inflammation in the face of challenge with IVAG WT HSV-2 (Fig. 1A and B), whereas nonimmune mice showed rapid replication of the virus in the vaginal epithelium (Fig. 1C), followed by the development of purulent genital lesions, hind-limb paralysis, and death (Fig. 1A and B). The paralysis and death associated with viral replication in the central nervous system, as seen here, are consistent with the findings in a well-established genital herpes mouse infection model (27). In contrast, although the i.p.-immunized mice all survived without hind-limb paralysis (Fig. 1A and B), they all had purulent genital lesions (clinical score = 3) (Fig. 1B). Viral titers in the vaginal wash of i.n.-immunized mice started to decrease on day 3 p.c., whereas the viral titers in i.p.-immunized mice did not decrease until day 5 (Fig. 1C). The differences in viral titer between the i.n.- and i.p.-immunized groups were not statistically significant ($P = 0.056$ on day 3 p.c. and $P = 0.200$ on day 4), and similar results were obtained in three different experiments. Histopathological analysis of the vaginas of these mice on day 8 p.c. revealed that i.p.-immunized mice had greater shedding of the vaginal epithelium through infection than did i.n.-immunized mice (Fig. 1D); this was consistent with the clinical score results (Fig. 1B). Therefore, i.n.-immunized mice were able to develop antiviral immunity at the infection site earlier than did i.p.-immunized mice and were protected from both vaginal inflammation and death; we define this as full protective immunity.

Nasally administered HSV-2 TK^- proliferates in the nasal cavity but not in the draining lymph nodes. Because i.n. live HSV-2 TK^- vaccination induced full protective immunity (Fig. 1), we next examined whether i.n. immunization with equivalent multiplicities of infection (MOI) (10^5 PFU) of heat-inactivated HSV-2 TK^- could induce protective immunity. All mice given heat-inactivated HSV-2 TK^- i.n. failed to survive WT HSV-2 challenge, as did nonimmune mice (data not shown), indicating that the live form of HSV-2 TK^- was required to induce protective immunity.

We next examined whether HSV-2 TK^- replicated in the nasal cavity to initiate an Ag-specific immune response. Nasal washes of mice immunized i.n. with HSV-2 TK^- were collected at various time points, and the viral titers were measured. Administered HSV-2 TK^- was first detected in the nasal washes at 3 h p.i.; the viral titer then started to decrease, probably because some of the inoculant was washed out by nasal flow. However, the titer then started to increase again sometime between 24 and 48 h p.i. (Fig. 2A), suggesting that viral replication was occurring in the nasal cavity.

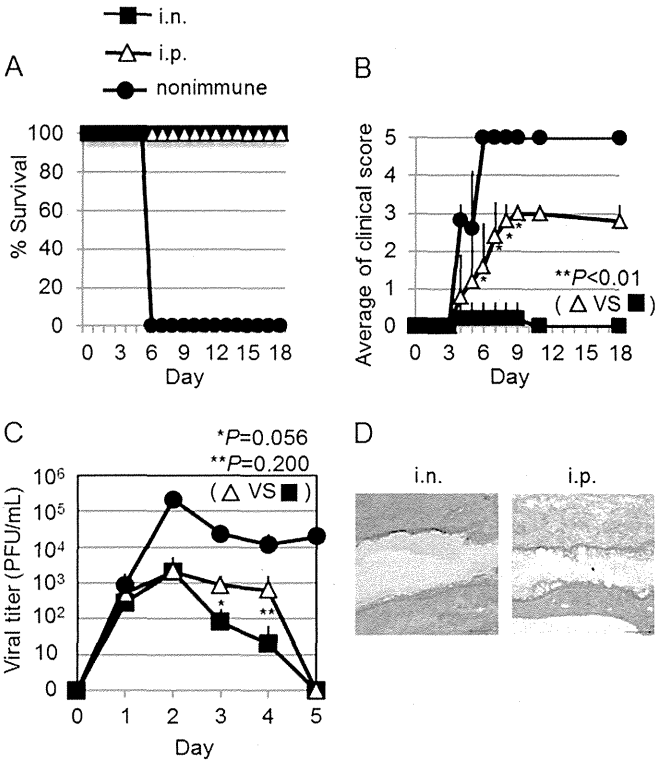

FIG 1 I.n. immunization with live HSV-2 TK^- induces protective immunity against IVAG WT HSV-2 challenge. Groups of five mice were immunized by a single i.n. or i.p. inoculation with 10^5 PFU of live HSV-2 TK^-. Three weeks postimmunization, the mice were challenged IVAG with 5×10^4 PFU of WT HSV-2. (A and B) Survival rates (A) and genital pathology scores (B) after IVAG HSV-2 challenge. (B) Disease severity was scored as follows (5): 0, no sign; 1, slight genital erythema and edema; 2, moderate genital inflammation; 3, purulent genital lesions; 4, hind-limb paralysis; and 5, moribund. $P < 0.01$ for the i.n.- versus the i.p.-immunized group for days 6 to 9 p.c. (C) Viral titers from vaginal washes collected at the indicated time points p.c. with IVAG WT HSV-2. $P = 0.056$ on day 3 and $P = 0.200$ on day 4 for the i.n.- versus the i.p.-immunized group. (D) Hematoxylin and eosin staining of the vaginal tissues of each group of mice at day 8 p.c. The error bars represent means ± SD of the number of mice per group. (A to D) The results are representative of three similar experiments.

To examine whether administered virus could reach the dLNs, we performed PCR for virus-specific DNA by using HSV-2 gB-specific primers (20). With this sensitive PCR method, which can detect a single copy of HSV-2-derived DNA (Fig. 2B), no HSV-2-derived DNA was detected in the cLNs (i.e., the dLNs of the nasal tissue) of i.n.-immunized mice for at least 72 h p.i. (Fig. 2C). In contrast, in the nasal passages, virus-specific DNA was detectable from 24 h until 72 h p.i. (Fig. 2C), supporting the results of the viral titer analysis (Fig. 2A). Therefore, i.n.-administered HSV-2 TK^- proliferates in the nasal cavity, but not in the cLNs. In addition, virus-specific DNA was not detected in the dorsal root ganglion (Fig. 2D), where latent HSV-2 is generally observed (1).

Effector CD4 T cells are generated by Ag-delivering nasal dendritic cells in the cervical lymph nodes and acquire the ability to migrate into systemic tissue. IVAG immunization with the same attenuated strain of HSV-2 that we used here induces pro-

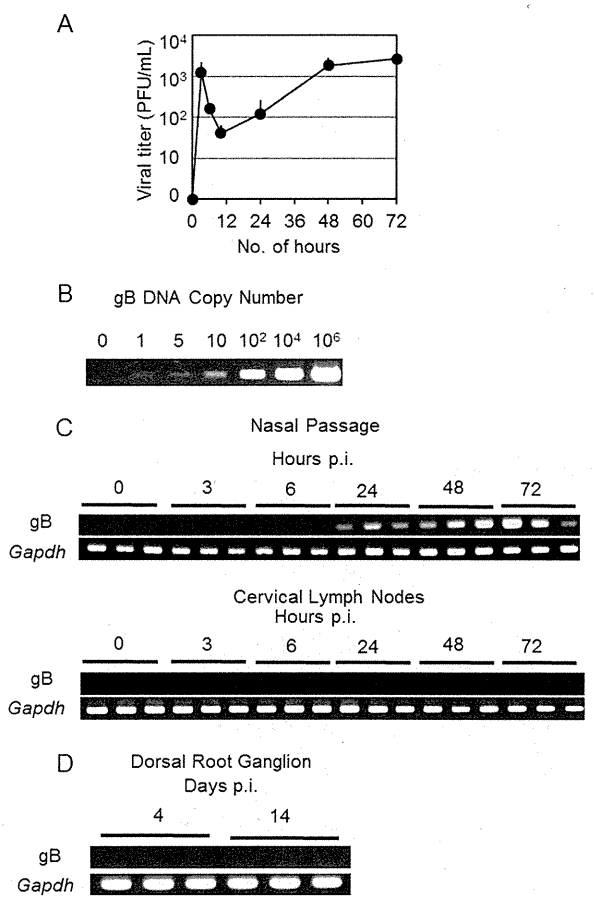

FIG 2 HSV-2 TK$^-$ given intranasally proliferates in the nasal cavity but not in the cervical lymph nodes. Mice in groups of three were each immunized with a single intranasal dose of 10^5 PFU of live HSV-2 TK$^-$. (A) Viral titers in nasal washes were measured at the indicated times after immunization. (C and D) PCR analysis for virus-derived DNA in the nasal passages (C), cervical lymph nodes (C), and dorsal root ganglion (D) using HSV-2 gB-specific primers. To normalize the tissue content for each sample, we detected the housekeeping gene *Gapdh*. (B) To confirm the sensitivity of the PCR analysis with gB-specific primers, PCR was performed with serially diluted gB-coding plasmid DNA. (A to D) The results are representative of three similar experiments.

tective immunity that is mediated by several types of effector cell, including CD4 T cells, CD8 T cells, and Ab-secreting cells; the most crucial type of cell is the CD4 T cell (21, 28–30). To address whether CD4 T cells are critical for early virus clearance following WT IVAG HSV-2 challenge in i.n.-immunized mice, depletion antibodies were i.p. injected a total of four times over the period from 4 days before to 2 days after infection (Fig. 3A). None of the CD4$^+$ cell-depleted i.n.-immunized mice survived after IVAG challenge with WT HSV-2 (Fig. 3B). In contrast, both CD8-depleted mice and natural killer (NK) cell-depleted mice survived and recovered from moderate or mild vaginal inflammation (Fig. 3C); this finding was similar to previous findings of a requirement for CD4 T cells in protective immunity against IVAG WT HSV-2 challenge in IVAG-immunized mice (21, 28–30).

Because we had confirmed that CD4 T cells were crucial for inducing protective immunity against IVAG WT HSV-2 challenge in i.n.-immunized mice, we next evaluated the place of antigen presentation in the generation of HSV-2-specific CD4 T cells. To address this issue, we performed *in vitro* culture of CD4 T cells collected from the cLNs or iliac lymph nodes (iLNs) (i.e., the dLNs of the vaginal tissue) of mice immunized i.n. with HSV-2 TK$^-$ at various time points. These CD4 T cells were stimulated with HSV-2 Ags *in vitro*. HSV-2-specific IFN-γ-secreting CD4 T cells (effector CD4 T cells) appeared at day 4 p.i. in the cLNs, whereas in the iLNs, the appearance of the effector CD4 T cells was delayed to day 7 p.i. (Fig. 4A).

We next examined whether HSV-2 Ag-presenting DCs were present in these LNs. DCs prepared from these LNs from i.n.-immunized mice at various time points were cocultured with HSV-2-specific CD4 T cells with or without the addition of HSV-2 Ags to the *in vitro* culture. The DCs prepared from cLNs had the ability to induce HSV-2-specific CD4 T cells to secrete IFN-γ without the addition of antigen (Fig. 4B), indicating that the DCs had captured HSV-2 Ags from the nasal cavity and migrated to the cLNs in 2 days, because we had already shown that viral DNA was not detectable in the cLNs (Fig. 2C). In contrast, DCs prepared from iLNs did not induce HSV-2-specific CD4 T cells to secrete IFN-γ above background levels at any time point. Thus, nasal DCs migrate and present viral Ags to naïve CD4 T cells in the cLNs, but not in the iLNs; we speculate that HSV-2-specific CD4 T cells are generated in the cLNs and then migrate into the systemic tissues, such as iLNs.

Intranasal immunization induces the accumulation of CD4 T cells in the vaginal mucosa for the induction of protective immunity with limited proliferation of CD4 T cells following IVAG infection with HSV-2. We next performed an adoptive-transfer experiment with a previously reported modified protocol (25) using effector CD4 T cells prepared from cLNs to examine whether these cells were able to migrate into the vaginal mucosa. C57BL/6 mice (CD45.2) received CD4 T cells from the cLNs of C57BL/6-Ly5.1 congenic mice (CD45.1) that were unimmunized or had been immunized with i.n. HSV-2 TK$^-$ 7 days previously. Two hours after the adoptive transfer, the C57BL/6 mice were challenged IVAG with WT HSV-2, and donor-derived CD45.1$^+$ CD4 T cell accumulation in the vaginal mucosa was examined by immunohistochemistry. CD45.1$^+$ donor-derived CD4 T cell accumulation was observed on day 3 p.c. in the submucosal region of the vaginal tissues of the mice that had received CD4 T cells prepared from mice immunized i.n. with HSV-2 TK$^-$ but not in that of naïve CD45.1$^+$ CD4 T cell-transferred mice (Fig. 5A, left and middle). We also performed a similar experiment with CD4 T cells prepared from the periportal LNs (i.e., the dLNs associated with the area of i.p. immunization) of i.p.-immunized mice. We found that CD4 T cells, which were able to migrate into the vaginal mucosa, were generated in the periportal LNs of i.p.-immunized mice (Fig. 5A, right).

I.n. immunization thus generated effector CD4 T cells in the cLNs that were able to migrate to peripheral tissues, such as the iLNs and vaginal mucosa (Fig. 5A). We next examined whether i.n. immunization induced the formation of an effector T cell pool in the vaginal mucosa. Without IVAG challenge, the total number of CD4 T cells in the vaginal mucosae of mice immunized i.n. with HSV-2 TK$^-$ 3 weeks previously did not differ significantly from that in unimmunized mice (Fig. 5B). After HSV-2 IVAG challenge, the total numbers of vaginal CD4 T cells in i.n.-immunized mice increased significantly (from about 2,200 to 14,300), whereas in i.p.-immunized mice they did not (from about 1,270 to 2,540) (Fig. 5B). We then performed a BrdU incorporation assay to determine the percentages of CD4 T cells that were proliferating. The

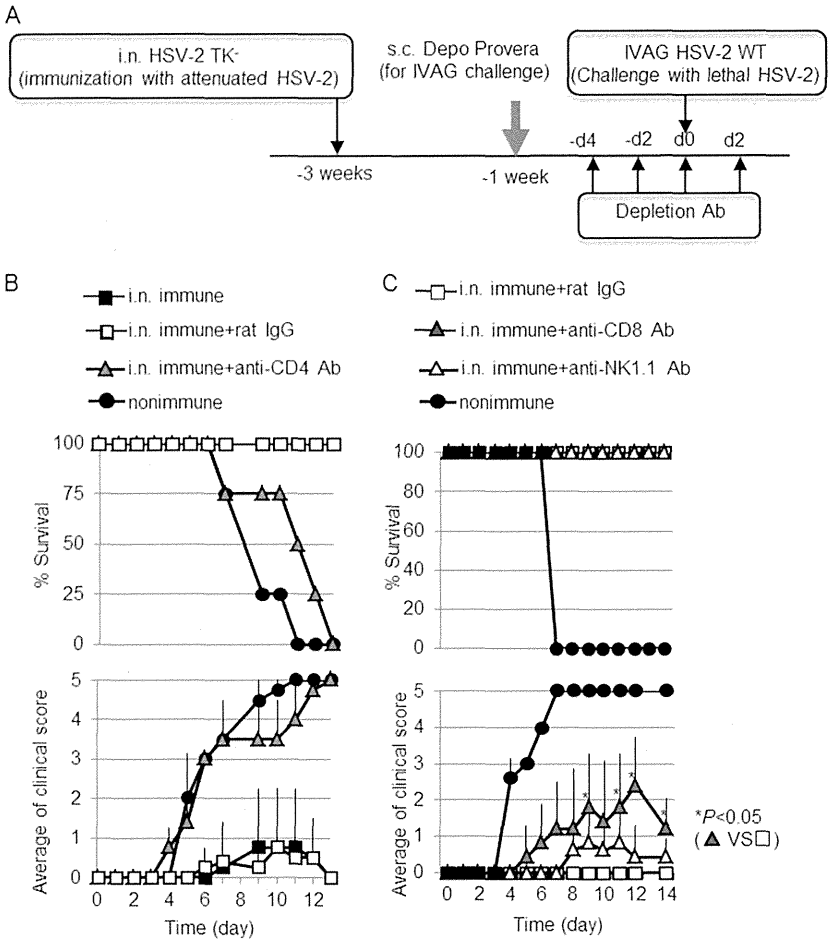

FIG 3 CD4 T cells, but not CD8 T cells and NK cells, are critical for the induction of protective immunity in mice immunized intranasally with HSV-2 TK$^-$ against IVAG WT HSV-2 challenge. (B and C) Mice in groups of four (B) or five (C) were immunized with a single i.n. dose of 10^5 PFU of HSV-2 TK$^-$. Three weeks postimmunization, the mice were challenged IVAG with 5×10^4 PFU of WT HSV-2. CD4 T cells (B), CD8 T cells (C), or NK cells (C) were depleted from the respective groups of mice by four injections of 100 μg of each depletion Ab given before and after the IVAG HSV-2 challenge, as shown in panel A. Anti-CD4 (GK1.1), anti-CD8a (53-6.7), and anti-NK1.1 (PK136) Abs that were used for the experiments were purified from the supernatant of hybridoma culture. Survival rates and genital pathology scores after IVAG HSV-2 challenge are depicted. The results are representative of three similar experiments. d, day; s.c., subcutaneous. The error bars indicate SD.

absolute numbers of proliferating and nonproliferating cells were calculated on the basis of the total cell numbers and the percentages of CD4$^+$ BrdU$^+$ cells or CD4$^+$ BrdU$^-$ cells, respectively, in the vaginal tissue. The percentages of CD4$^+$ BrdU$^+$ cells or CD4$^+$ BrdU$^-$ cells were determined by fluorescence-activated cell sorter (FACS) analysis (data not shown). The assay revealed that <10% of vaginal CD4 T cells in all groups of mice were proliferating (Fig. 5B). In line with these findings, our immunohistochemistry data suggested that most CD4 T cells were Ki-67 negative, whereas Ki-67-positive cells were present in the epithelial layer (Fig. 5C).

To examine whether the effector T cells induced by i.n. immunization in the cLNs were protective against IVAG HSV-2 challenge, we next performed an IVAG HSV-2 challenge experiment in mice to which we had adoptively transferred whole cLN cells or CD4 T cells alone from mice immunized with i.n. HSV-2 TK$^-$. Mice to which we had adoptively transferred whole cLN cells from immunized mice survived without severe vaginal inflammation in the face of challenge with 10^3 PFU (1.6 LD_{50}) of IVAG WT HSV-2. In contrast, mice that received cells from unimmunized donors all died after the development of high viral titers in vaginal washes, along with purulent genital lesions and hind-limb paralysis (Fig. 6A). Unlike the mice that had received whole cLN cells from i.n.-immunized mice, mice to which we had adoptively transferred CD4 T cells alone were not protected (Fig. 6B). Thus, HSV-2-specific CD4 T cells alone prepared from the cLNs of i.n.-immunized mice were not sufficient for protection; the help of other cell types was perhaps required.

Intranasal immunization with HSV-2 TK$^-$ induces long-lasting retention of HSV-2-specific IFN-γ-secreting effector T cells in the vaginal tissues. The findings described above led us to measure the numbers of HSV-2-specific effector T cells. HSV-2-specific IFN-γ-secreting cells were detected in the vaginas of i.n.-immunized mice at 3 weeks (Fig. 7A) and 6 weeks (data not shown) p.i. without IVAG HSV-2 challenge; the numbers of these cells were minimal in the vaginas of i.p.-immunized mice, although similar levels of effector T cells were detected in the spleens of i.p.- and i.n.-immunized mice at 1 and 3 weeks p.i. (Fig. 7A and B). Interestingly, HSV-2-specific effector T cells appeared at 1

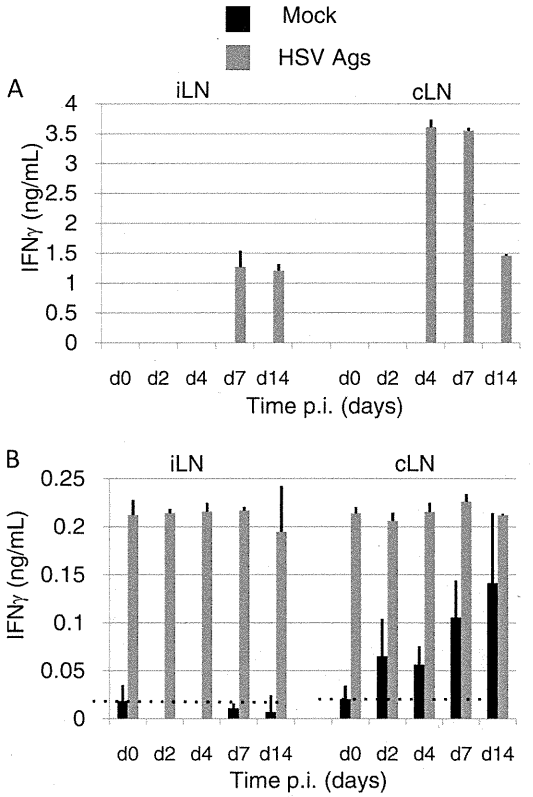

FIG 4 Effector CD4 T cells are generated by antigen-harboring dendritic cells in the cLNs and acquire the ability to migrate into systemic tissues. (A) $CD4^+$ cells were isolated at the time points indicated on the *x* axis from the cLNs or iLNs of mice immunized with HSV-2 TK^- and stimulated with antigen-presenting cells in the absence or presence of added heat-inactivated virus. IFN-γ secreted from T cells was measured by ELISA. (B) $CD11c^+$ cells were isolated at the time points indicated on the *x* axis from the cLNs or iLNs of mice immunized intranasally with HSV-2 TK^-. The cells were then cocultured with CD4 T cells isolated from the cLNs of mice immunized i.n. 7 days previously with HSV-2 TK^- (i.e., HSV-specific CD4 T cells) in the absence or presence of added heat-inactivated virus. IFN-γ secreted from T cells was measured by ELISA. (A and B) The results are representative of three similar experiments. d, day. The error bars indicate SD.

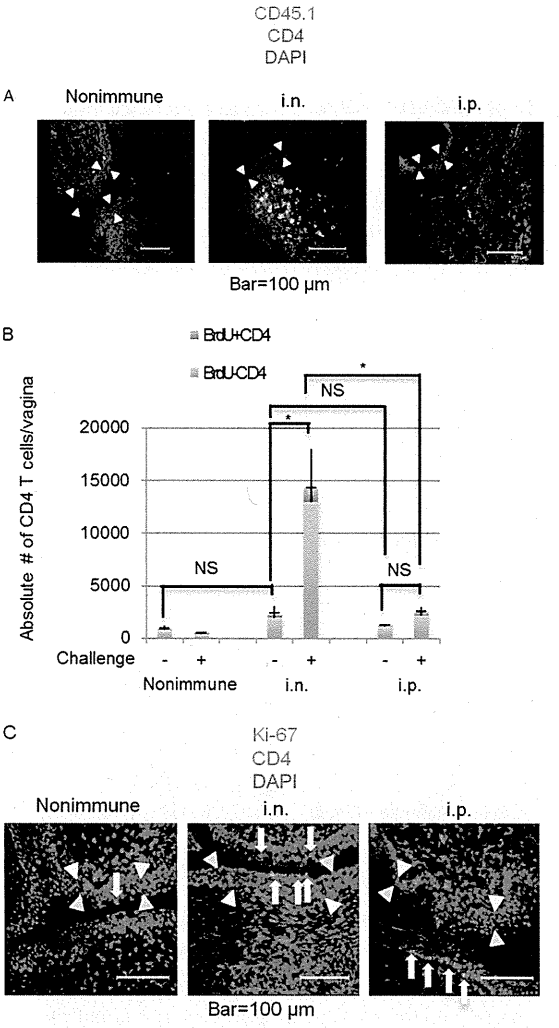

FIG 5 Mice immunized intranasally with HSV-2 TK^- have increased numbers of nonproliferating CD4 T cells in their vaginal tissues following IVAG infection with HSV-2. (A) CD4 T cells isolated from the cervical lymph nodes of i.n.-immunized mice or unimmunized congenic mice or from the peripportal lymph nodes of i.p.-immunized congenic mice (CD45.1) were adoptively transferred to C57BL/6 mice (CD45.2), which were then challenged IVAG with WT HSV-2. After 3 days, CD4 T cells (anti-CD4; red), donor-derived cells (anti-CD45.1; green), and nuclei (DAPI [4′,6-diamidino-2-phenylindole]; blue) were visualized. The epithelial layer is indicated by yellow arrowheads (luminal edge) and white arrowheads (basement membrane). (B and C) Three mice in each group were immunized with a single i.n. or i.p. dose of 10^5 PFU of HSV-2 TK^-. Three weeks postimmunization, the mice were challenged IVAG with 5×10^4 PFU of WT HSV-2. (B) At day 0 (challenge −) and day 1 (challenge +) after IVAG challenge with HSV-2, the percentage of proliferating CD4 T cells in the vaginal tissues was determined by BrdU incorporation assay. Absolute numbers of proliferating and nonproliferating cells were calculated on the basis of the total cell number and the percentage of $CD4^+$ $BrdU^+$ cells or $CD4^+$ $BrdU^-$ cells, respectively, in the vaginal tissue. The capped error bars relate to $BrdU^+$ cells, and the uncapped error bars relate to $BrdU^-$ cells (indicating SD). Statistical analysis was done on the total numbers of CD4 T cells. *, $P < 0.05$; NS, not significant. (C) At day 1 after IVAG challenge with WT HSV-2, CD4 T cells (anti-CD4; red) and proliferating cells (Ki-67; green) in the vaginal tissues were visualized. The arrows point to Ki-67-positive cells. (A to C) The results are representative of three similar experiments.

week p.i. in the vaginas of i.p.-immunized mice (Fig. 7B), although their levels were significantly lower than those in the vaginas of i.n.-immunized mice, indicating that the effector T cells generated in the i.p.-immunized mice could migrate into, but were not retained in, the vaginal tissues. Thus, i.n.-immunized mice generated and maintained an HSV-2-specific effector T cell pool for at least 6 weeks in the vaginal mucosa; this was not the case with HSV-2-specific effector T cells in i.p.-immunized mice. As well as inducing the early development of an HSV-2-specific effector T cell pool in the vaginal tissues (Fig. 7B), i.n. HSV-2 TK^- vaccination resulted in prolonged retention of the effector T cell pool in the reproductive mucosa.

Next, we examined whether the number of HSV-2-specific effector T cells in the vaginas of the mice in each group was affected by the stimulation of IVAG WT HSV-2 challenge. The number of HSV-2-specific IFN-γ-secreting cells in the vaginas of i.n.-immunized mice was about 100 before challenge (Fig. 7A); it increased to about 350 on day 1 p.c. and 500 on day 3 p.c. (Fig. 7C). In contrast, i.p.-immunized mice showed a slow increase in the number of vaginal HSV-2-specific IFN-γ-secreting cells (from about

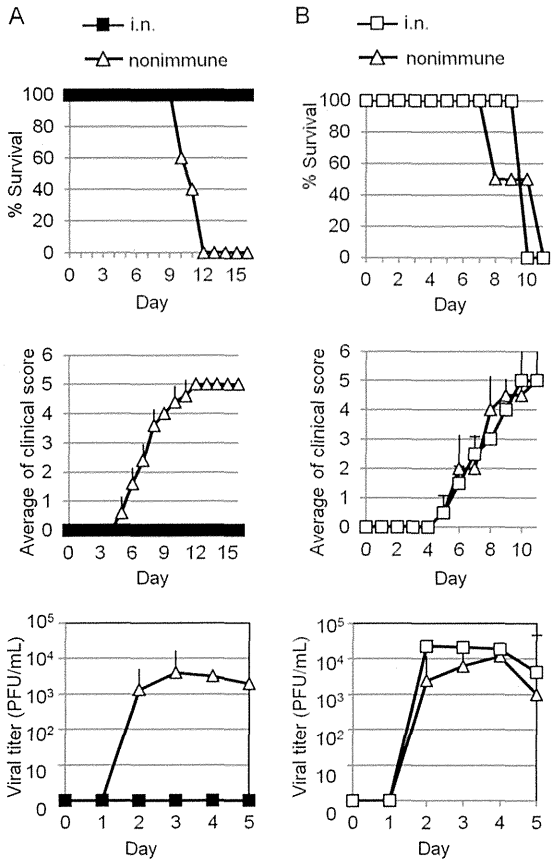

FIG 6 Effector cells generated in i.n.-immunized mice are protective against IVAG challenge with WT HSV-2. Whole cells (A) or CD4 T cells (B) isolated from the cervical lymph nodes of i.n.-immunized or unimmunized C57BL/6 mice were adoptively transferred to naïve C57BL/6 mice, which were then challenged IVAG with WT HSV-2 at 10^3 PFU (1.6 LD_{50}) on day 4 after the adoptive transfer. Survival rates, genital pathology scores, and viral titers in vaginal washes after IVAG HSV-2 challenge are depicted as described in the legend to Fig. 1. (A and B) The results are representative of two separate experiments. The error bars indicate SD.

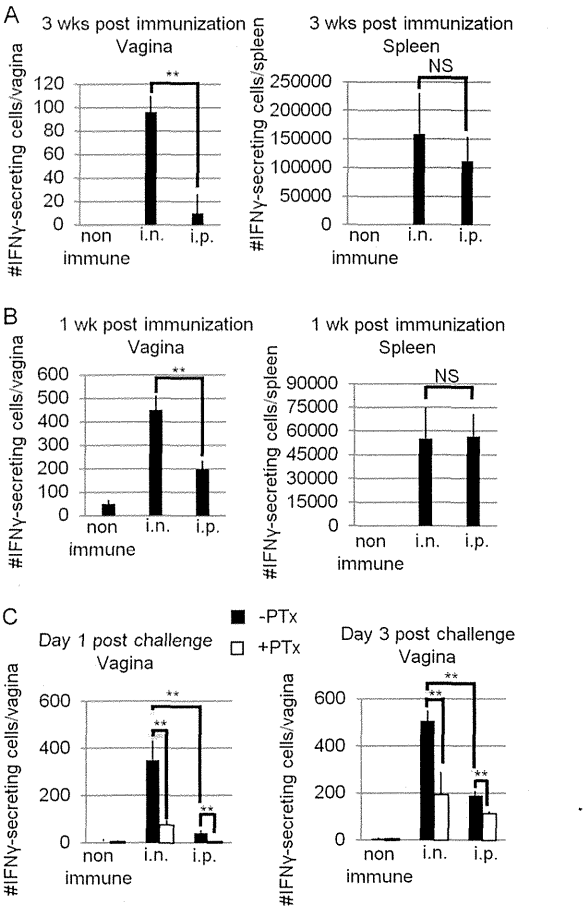

FIG 7 Mice immunized intranasally with HSV-2 TK^- have HSV-2-specific IFN-γ-secreting cells, not only in the systemic compartment, but also in the vaginal tissues. Three mice in each group were immunized with a single i.n. or i.p. dose of 10^5 PFU of HSV-2 TK^-. (C) Three weeks p.i., the mice were challenged IVAG with WT HSV-2 at 5×10^4 PFU. Whole cells prepared from the vaginal tissues or spleens of three mice in each group were pooled and stimulated for 72 h *in vitro* with irradiated syngeneic splenocytes as antigen-presenting cells in the presence of heat-inactivated virus antigens. The absolute numbers of IFN-γ-secreting cells in the vaginal tissues or spleen at 1 week p.i. (B), 3 weeks p.i. (A), and days 1 and 3 postchallenge (C) were calculated by ELISPOT assay. (C) Pertussis toxin (0.5 μg) was injected intraperitoneally 2 h before and 2 days after IVAG infection. (A to C) The results are representative of three similar experiments. The error bars indicate standard errors (SE) for three wells in the ELISPOT assay. **, $P < 0.01$; NS, not significant.

10 before challenge to 40 at day 1 p.c. and 190 at day 3 p.c.) (Fig. 7A and C).

To address whether the vaginal effector T cells detected in the two groups of mice were local resident effector T cells or migrant effector memory T cells from the systemic compartment, we examined the absolute numbers of HSV-2-specific IFN-γ-secreting cells in the vaginas of each group of mice injected with PTx, an inhibitor of Giα signaling, 2 h before and 2 days after IVAG WT HSV-2 challenge. PTx inhibits chemokine-induced lymphocyte migration (31). At 1 day p.c., after PTx treatment, the number of effector T cells in the vaginal mucosae of i.n.-immunized mice significantly decreased to levels similar to those seen in the mice before IVAG WT HSV-2 challenge (Fig. 7A); at the same time point, the vaginal effector T cells that had been observed in small numbers in i.p.-immunized mice had mostly disappeared upon PTx injection (Fig. 7C). These data revealed that the HSV-specific IFN-γ-secreting cells detected in the vaginas of i.n.-immunized mice included both local effector T cells retained in the vaginal mucosa after immunization and Giα signaling-dependent circulating memory cells that had migrated rapidly from the systemic compartment upon stimulation by IVAG WT HSV-2 challenge. In contrast, the HSV-2-specific IFN-γ-secreting cells detected in the vaginas of i.p.-immunized mice were mostly migrant circulating memory T cells.

Local effector T cells are critical for the induction of protective immunity against WT HSV-2 infection. We next examined the important issue of whether local effector T cells, circulating memory T cells, or both are prerequisites for protective immunity against IVAG WT HSV-2 infection. To examine the importance of circulating memory T cells migrating into the vagina early in infection, PTx was injected 2 days and 2 h before WT HSV-2 challenge. PTx injection of both i.n.-immunized mice and nonimmune mice did not affect survival rates or clinical scores (Fig. 8A). In contrast, i.p.-immunized mice injected with PTx started to develop vaginal inflammation earlier than did non-PTx-injected

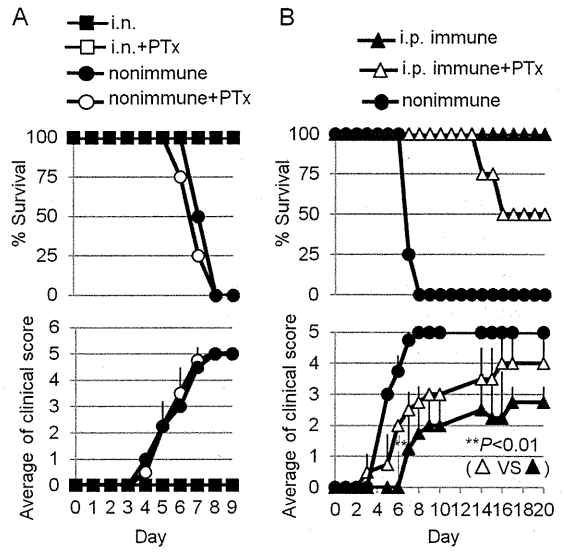

FIG 8 Local effector memory CD4 T cells are critical for the induction of protective immunity against IVAG WT HSV-2 challenge. Groups of four mice were immunized with a single i.n. (A) or i.p. (B) dose of 10^5 PFU of HSV-2 TK$^-$. Three weeks postimmunization, the mice were challenged IVAG with 5×10^4 PFU of WT HSV-2. Pertussis toxin (0.5 μg) was injected by the i.p. route 2 h and 2 days before IVAG infection. Survival rates and genital pathology scores after IVAG HSV-2 challenge are depicted. (A and B) The results are representative of two similar experiments. The error bars indicate SD.

mice, and 50% of the i.p.-immunized mice given PTx died (Fig. 8B). These data demonstrate that i.n. HSV-2 TK$^-$ vaccination induced the production of local effector T cells, which, in addition to the circulating memory T cell pool, contributed to early and prolonged protection against HSV-2. In contrast, i.p. immunization did not induce early protection owing to a lack of local vaginal effector T cell induction capacity; HSV-2-specific circulating memory T cells seemed to play a critical role in the protection provided by i.p. immunization.

DISCUSSION

Genital herpesvirus invades the host by establishing an infection in the vaginal epithelium before spreading to the central nervous system and establishing lifelong latency (1). Severe signs, such as hind-limb paralysis and death, are associated with virus replication in the peripheral nervous system in the genital herpes mouse model (27); we therefore used this model to elucidate the cellular mechanisms of induction of protective immunity against HSV by i.n. vaccination with live-attenuated HSV-2 TK$^-$. Local effector T cells in the vaginal mucosa are critical gatekeepers for rapid clearance of the invading HSV-2 at local infection sites by secreting IFN-γ (25). Our study showed that i.n. immunization with live-attenuated HSV-2 resulted in the induction of effector T cells and their migration to, and retention in, the vaginal mucosa (Fig. 7A and B). The effector T cells were retained for at least 6 weeks p.i. (data not shown), whereas systemic vaccination was barely able to establish a local effector cell pool, even when it induced the production of circulating memory T cells in the systemic compartment (Fig. 7A and B). Recently, a novel STD vaccine strategy combining systemic immunization and chemokine treatment of the vaginal mucosa was reported (12). This vaccine strategy solves the problem of the lack of generation of a local effector T cell pool by systemic vaccination by using the locally introduced chemokines CXCL9 and CXCL10 to direct circulating memory CD8 T cells to the vaginal mucosa (12). In our current study, vaccination with a single i.n. dose of live HSV-2 TK$^-$ induced both a local effector T cell pool in the vaginal mucosa and systemic memory T cells (Fig. 7) without the need for artificial chemokine treatment of the vaginal mucosa. The result was superior protection against IVAG WT HSV-2 challenge by the initiation of viral clearance at the vaginal mucosa earlier than with i.p. immunization (Fig. 1A, B, and C). Our experiments with PTx treatment, which inhibits chemokine-induced lymphocyte migration (31), revealed that local vaginal effector T cells are critical for rapid viral clearance (Fig. 8). In i.p.-immunized mice, a delayed migration of circulating memory T cells (at day 3 p.c.) from the systemic compartment to the vaginal mucosa was induced by IVAG WT HSV-2 challenge (Fig. 7C). However, these circulating memory T cells could not prevent severe vaginal inflammation (Fig. 1B), indicating that the presence of HSV-2-specific effector T cells locally soon after challenge is critical for rapid clearance of HSV-2 and prevention of severe vaginal inflammation. In addition to local effector T cells, rapid recruitment of circulating memory T cells was also observed at day 1 p.c. in i.n.-immunized mice; these further contributed to the improved clearance of HSV from the reproductive tissues compared with systemic vaccination (Fig. 7C). These findings, together with our finding that i.p.-immunized mice had circulating memory T cells that arrived at the vaginal tissues at 3 days p.c. (Fig. 7C) and eventually cleared the virus from the vaginal mucosa (Fig. 1C) and survived (Fig. 1A and 8B), suggest that circulating memory T cells also help to prevent proliferation of the virus and viral spread to the nervous system. This speculation is supported by our observation that inhibition of the migration of circulating memory T cells into the vaginal mucosa caused the virus to spread to the central nervous system in i.p.-immunized mice (Fig. 8B), even though the PTx treatment seems to be partially effective in the vagina, given the fact that increased numbers of HSV-2-specific effector T cells are observed in the vaginal mucosa in PTx-treated mice at day 3 p.c. (Fig. 7C).

Our *ex vivo* coculture experiments revealed that DCs, which can induce IFN-γ secreting HSV-2-specific CD4 T cells in the absence of exogenous Ags, were present in the cLNs of mice immunized i.n. with HSV-2 TK$^-$ (Fig. 4B). Because viral DNA was detected in the nasal passages, but not in the cLNs (Fig. 2C), these results suggest that nasal DCs deliver viral Ags from the nasal cavity to the cLNs and then present the Ags to naïve CD4 T cells. This observation confirms the results of previous reports showing that mucosally administered Ags do not access the dLNs (20, 32). In addition, we showed that i.n. immunization with heat-inactivated virus did not induce protective immunity against IVAG WT HSV-2 challenge (data not shown). It is unlikely that the heat-inactivated virus breaks the mucosal barrier and accesses the DCs residing in both the nasal epithelial layer and the submucosal region (33) or accesses the cLNs directly. Taken together, our results indicate that the cLNs are the location of Ag presentation by Ag-harboring nasal DCs in i.n.-immunized mice; the effector T cells generated there subsequently migrate to peripheral effector tissues, such as the vaginal mucosa.

By adoptive-transfer experiments, we showed that cLN cells prepared from i.n.-immunized mice protected against IVAG challenge with WT HSV-2 (Fig. 6A). However, interestingly, mice that received only CD4 T cells prepared from the cLNs of i.n.-immu-

nized mice did not survive IVAG HSV-2 challenge (Fig. 6B). These data suggest that recruitment of an HSV-2-specific CD4 T cell subset alone into the vaginal mucosa is insufficient to induce protective immunity in naïve mice. Iijima et al. (25) showed previously that DCs and B cells together are required for the recall response of tissue memory CD4 T cells against IVAG HSV-2 challenge. Because we showed here that DCs carrying HSV-2 Ags did not migrate to distant iLNs, we assume that adoptive transfer of HSV-2-specific CD4 T cells alone from i.n.-immunized mice is not sufficient for protection owing to a lack of other cell types—perhaps B cells, as mentioned above—cooperating with these CD4 T cells. In addition, a lack of HSV-specific CD8 T cells may have been a contributor to the deaths in our mice, because CD8 T cells seem to contribute to virus clearance: CD8-depleted mice developed mild vaginal inflammation upon IVAG HSV-2 challenge, although the mice survived (Fig. 3).

The mechanism by which i.n. immunization with live HSV-2 TK^- can induce the production of HSV-specific effector T cells and their long-lasting residence in the vagina, along with full protective immunity, is unknown. Previous studies have suggested that circulating memory CD8 T cells induced by systemic immunization with HSV-2 TK^- can be recruited to, and retained in, the vaginal mucosa by CXCL9 and CXCL10 chemokine treatment, but effector CD4 T cells cannot be retained for a long time (12). In our study, HSV-2-specific effector T cells were retained in the vaginal mucosae of i.n.-immunized mice (Fig. 7A). This finding suggests that the mechanism of retention of local effector CD4 T cells in the vagina involves an adhesion molecule, such as integrin, besides the previously reported Giα signaling-dependent chemokines CXCL9 and CXCL10 (12). Tissue-associated DCs are capable of imprinting the tropism of a T cell during the priming phase. For instance, DCs residing in Peyer's patches and the mesenteric lymph nodes induce T cells to express the gut-homing molecules integrin $\alpha4\beta7$ and CCR9 by providing retinoic acid (34, 35). More recently, in addition to this DC-mediated tissue imprinting, it has been demonstrated that the tissue microenvironment determines the tropism of effector T cells into the intestinal mucosa and their retention there (36–38). Transplantation of peripheral LNs into mesenteric lymphadenectomized mice fails to sustain gut-homing T cells, despite retinoic acid production by DCs migrating with Ags into the LNs (36). Moreover, a DC adoptive-transfer experiment revealed that induction of the production of tissue-specific homing molecules depends on the route of injection of transferred DCs, but not on their origin (37, 38). Thus, in addition to tissue-derived DCs, which can initiate the imprinting of tissue tropism of T cells, other types of cells, such as stromal cells or fibroblasts, are likely to be involved in tissue imprinting and retention processes. From our results, it is interesting to postulate that immunization with HSV-2 TK^- via a locally specific microenvironment (namely, the nasal epithelium) provides signals that support the induction and retention of vaginal-tissue-associated adhesion and chemokine molecules on HSV-2-specific effector CD4 T cells.

Our data provide the first evidence for the critical role played by nasal-immunization-induced local vaginal effector T cells in the development of protective immunity against genital virus infection. A further understanding of the mechanisms of cross talk between infected nasal epithelium and antigen-specific immune cells in inducing the production of effector cells and their local retention in the distant vagina and of the safety aspect of the i.n.-vaccination strategy is key to the design of vaccines that induce optimal effector immunity.

ACKNOWLEDGMENTS

We thank David Knipe (Harvard Medical School, Boston, MA) for providing HSV-2 strains $186syn^+$ and $186TK^-$.

A. Sato was a Japan Society Promotion of Science (JSPS) fellow. This work is supported by grants from the Ministry of Education, Culture, Sports, Science, and Technology of Japan (Grant-in-Aid for Scientific Research S [23229004]) and the Core Research for Evolutional Science and Technology Program of the Japan Science and Technology Agency and by a Health Labor Sciences Research Grant from the Ministry of Health, Labor and Welfare of Japan.

We have no conflicting financial interests.

REFERENCES

1. **Roizmam B, Knipe D, Whitley RJ.** 2007. Herpes simplex viruses, p 2502–2601. *In* Knipe DM, Howley PM, Griffin DE, Lamb RA, Martin MA, Roizman B, Straus SE. (ed), Fields virology, 5th ed. Lippinott-Williams & Wilkins, Philadelphia, PA.
2. **Langenberg AG, Burke RL, Adair SF, Sekulovich R, Tigges M, Dekker CL, Corey L.** 1995. A recombinant glycoprotein vaccine for herpes simplex virus type 2: safety and immunogenicity. Ann. Intern. Med. **122**:889–898. http://dx.doi.org/10.7326/0003-4819-122-12-199506150-00001.
3. **Bourne N, Milligan GN, Schleiss MR, Bernstein DI, Stanberry LR.** 1996. DNA immunization confers protective immunity on mice challenged intravaginally with herpes simplex virus type 2. Vaccine **14**:1230–1234. http://dx.doi.org/10.1016/S0264-410X(96)00027-8.
4. **Kuklin N, Daheshia M, Karem K, Manickan E, Rouse BT.** 1997. Induction of mucosal immunity against herpes simplex virus by plasmid DNA immunization. J. Virol. **71**:3138–3145.
5. **Morrison LA, Da Costa XJ, Knipe DM.** 1998. Influence of mucosal and parenteral immunization with a replication-defective mutant of HSV-2 on immune responses and protection from genital challenge. Virology **243**:178–187. http://dx.doi.org/10.1006/viro.1998.9047.
6. **Gallichan WS, Rosenthal KL.** 1998. Long-term immunity and protection against herpes simplex virus type 2 in the murine female genital tract after mucosal but not systemic immunization. J. Infect. Dis. **177**:1155–1161. http://dx.doi.org/10.1086/515286.
7. **Corey L, Langenberg AG, Ashley R, Sekulovich RE, Izu AE, Douglas JM, Jr, Handsfield HH, Warren T, Marr L, Tyring S, DiCarlo R, Adimora AA, Leone P, Dekker CL, Burke RL, Leong WP, Straus SE.** 1999. Recombinant glycoprotein vaccine for the prevention of genital HSV-2 infection: two randomized controlled trials. Chiron HSV Vaccine Study Group. JAMA **282**:331–340.
8. **Brockman MA, Knipe DM.** 2002. Herpes simplex virus vectors elicit durable immune responses in the presence of preexisting host immunity. J. Virol. **76**:3678–3687. http://dx.doi.org/10.1128/JVI.76.8.3678-3687.2002.
9. **Koelle DM, Corey L.** 2008. Herpes simplex: insights on pathogenesis and possible vaccines. Annu. Rev. Med. **59**:381–395. http://dx.doi.org/10.1146/annurev.med.59.061606.095540.
10. **Parr MB, Parr EL.** 2003. Vaginal immunity in the HSV-2 mouse model. Int. Rev. Immunol. **22**:43–63. http://dx.doi.org/10.1080/08830180305228.
11. **McElrath MJ, Haynes BF.** 2010. Induction of immunity to human immunodeficiency virus type-1 by vaccination. Immunity **33**:542–554. http://dx.doi.org/10.1016/j.immuni.2010.09.011.
12. **Shin H, Iwasaki A.** 2012. A vaccine strategy that protects against genital herpes by establishing local memory T cells. Nature **491**:463–467. http://dx.doi.org/10.1038/nature11522.
13. **Gebhardt T, Wakim LM, Eidsmo L, Reading PC, Heath WR, Carbone FR.** 2009. Memory T cells in nonlymphoid tissue that provide enhanced local immunity during infection with herpes simplex virus. Nat. Immunol. **10**:524–530. http://dx.doi.org/10.1038/ni.1718.
14. **Masopust D, Choo D, Vezys V, Wherry EJ, Duraiswamy J, Akondy R, Wang J, Casey KA, Barber DL, Kawamura KS, Fraser KA, Webby RJ, Brinkmann V, Butcher EC, Newell KA, Ahmed R.** 2010. Dynamic T cell migration program provides resident memory within intestinal epithelium. J. Exp. Med. **207**:553–564. http://dx.doi.org/10.1084/jem.20090858.
15. **Klonowski KD, Williams KJ, Marzo AL, Blair DA, Lingenheld EG,**